NASA TECHNICAL NOTE

NASA TN D-5075

NASA TN D-5075

TRANSMISSION OF 2.43 MeV ELECTRONS THROUGH THICK SILICON TARGETS

by Jag J. Singh

Langley Research Center
Langley Station, Hampton, Va.

NATIONAL AERONAUTICS AND SPACE ADMINISTRATION • WASHINGTON, D. C. • FEBRUARY 1969

NASA TN D-5075

TRANSMISSION OF 2.43 MeV ELECTRONS THROUGH THICK SILICON TARGETS

By Jag J. Singh

Langley Research Center
Langley Station, Hampton, Va.

NATIONAL AERONAUTICS AND SPACE ADMINISTRATION

For sale by the Clearinghouse for Federal Scientific and Technical Information
Springfield, Virginia 22151 – CFSTI price $3.00

TRANSMISSION OF 2.43 MeV ELECTRONS THROUGH THICK SILICON TARGETS

By Jag J. Singh
Langley Research Center

SUMMARY

The energy and angular distribution of electrons transmitted through silicon targets of various thicknesses have been measured for perpendicularly incident electrons of energy 2.43 MeV. The transmitted electron spectra were measured with 5-mm deep lithium-drifted silicon detectors. The experimental results have been compared with the Monte Carlo results obtained by Berger and Seltzer. The Monte Carlo program includes the effects of secondary electrons and photons and also the effects of ionization energy-loss fluctuations. The inclusion of these effects in the theoretical calculations has reduced the discrepancy between the theory and the experiment considerably. The target thickness at which the average cosine of the deflection angles reaches its asymptotic value is measured to be 2.5 ± 0.1 millimeters for 2.43 MeV electrons normally incident on plane parallel silicon targets.

INTRODUCTION

There has been a noticeable discrepancy between the experimental results and the theoretical calculations of the multiple scattering of electrons in extended media. (See refs. 1 to 8.) Complications arise from the statistical nature of the ionization energy loss and the complexity of the effective coulomb interaction between the incident electrons and the screened atomic field. In principle, one should be able to solve the transport problem exactly if the screening effects of the atomic electrons and the single scattering law of the incident relativistic electrons are known precisely. However, this approach will involve long and tedious calculations on a computer, and, in any case, the large angle scattering at moderate energies involve complex boundary conditions and path-length problems which are only partially solvable at present. Consequently, theoretical electron transport calculations usually have been made with various degrees of simplification. The main purpose of the measurements reported here has been to provide experimental check on the Monte Carlo transport calculations from an angular and spectral distribution standpoint for a specific source-medium configuration, namely, normal incidence. As a result, these measurements have emphasized the spectral distribution and the angular distribution of the transmitted electrons, as opposed to absolute measurements. On the basis of such a comparison at several electron energies, one should be able to write a computer code that predicts the experimental results with a good degree of accuracy. These measurements can also be used as reference data to check the adequacy of calculational techniques for more complex engineering shields.

EXPERIMENTAL PROCEDURE

Figure 1 shows the experimental arrangement used in these measurements. The Faraday cup and the fixed detector were used to monitor the number of electrons incident on the target during the angular distribution measurements of the transmitted electrons. A well collimated, narrow, electron beam of energy (2430 ± 5 keV) from an electrostatic generator was allowed to fall on a 2-centimeter-diameter silicon target. The beam spot on the target was a circle with a diameter of about 2 millimeters. The silicon target thickness ranged from 10 percent to 50 percent of the range of the incident electrons in the continuous slowing down approximation (designated CSDA). The transmitted electron spectra were measured with a well shielded and well collimated 5-millimeter-thick 80-millimeter^2-area, planar lithium-drifted silicon detector. (See refs. 1 and 2 for details of detector assembly.) Spectra were measured with and without a 5-mm-thick aluminum disk in front of the detector assembly. This technique enabled us to allow for the X-ray contribution from the target and other sources. The detectors were calibrated by use of Cs^{137} and Bi^{207} electron sources. Figure 2 shows the conversion electron spectra from these sources.

Figure 3 shows the spectra of monoenergetic electrons scattered from a 100-μg/cm^2-thick gold target. Notice the steady increase[1] in the full width at half the maximum height (designated FWHM) of the scattered electron peaks as well as the

---

[1]It must be pointed out that the effect of increased radiation detector variance at higher electron energies is expected to be negligible on the overall system resolution. For instance,

$$(\mathrm{FWHM})^2_{\mathrm{overall}} = (\mathrm{FWHM})^2_{\mathrm{elec}} + (\mathrm{FWHM})^2_{\mathrm{det\text{-}stat}}$$

$$(\mathrm{FWHM})^2_{\mathrm{overall}} = (\mathrm{FWHM})^2_{\mathrm{elec}} + (2.35)^2 FE\epsilon$$

where

F Fano factor, ($0 < F < 1$; ≈ 0.1 for silicon)

E energy of incident electrons

ϵ energy required to produce an electron-hole pair (≈ 3.6 eV for silicon)

$$(\mathrm{FWHM})^2_{\mathrm{overall}} = \left[(\mathrm{FWHM})^2_{\mathrm{elec}} + 2 \times 10^6\right] (\text{electron volts})^2 \quad (E = 1 \text{ MeV})$$

$$(\mathrm{FWHM})^2_{\mathrm{overall}} = \left[(\mathrm{FWHM})^2_{\mathrm{elec}} + 4 \times 10^6\right] (\text{electron volts})^2 \quad (E = 2 \text{ MeV})$$

It is obvious that the effect of statistical fluctuations in the number of carrier pairs produced by the incident radiation on the overall system resolution is negligible excepting in cases where the $(\mathrm{FWHM})_{\mathrm{elec}}$ is comparable to the detector variance. The electronic system used in the present investigation had an $(\mathrm{FWHM})_{\mathrm{elec}}$ of 10 keV.

nonzero number of counts in the channels below the peak position. The former is probably due to the combined effects of the slightly increased energy uncertainty at higher electron energies and poorer resolving power of the detectors for higher energy electrons whereas the latter results from electron backscattering from the silicon detector. Figure 4 shows the resolving power of the detection system as a function of the incident electron energy. Beyond an electron energy of 1500 keV, the FWHM rises steadily, although slowly, with the electron energy. Figure 5 shows the ratio of peak intensity to total area under spectrum as a function of the energy of the electrons incident on the gold target. The information contained in figures 4 and 5 is needed to introduce the effects of the finite resolving power of the detection system and the backscattering from the detector material on the Monte Carlo histograms. These histograms have to be corrected for the resolution of the detection system before a comparison with the experimental spectra can be made. Figure 6 shows the manner in which these effects are introduced. As seen in the insert, a Gaussian peak with an appropriate "tail" is drawn so that the area under the histogram matches that under the Gaussian pulse. This process is repeated for each energy interval and a final resultant curve is drawn to represent the complete histogram as shown in the figure.

THEORETICAL CALCULATIONS

The theoretical calculations are made by assuming a broad incident electron beam on infinitely wide plane parallel targets. This configuration corresponds very closely to the experimental conditions where the lateral dimension of the target is much greater than the incident electron range as well as the beam spot size. The details of the calculational procedure are described below.

Ten thousand normally incident electrons are allowed to enter the plane parallel slabs which are finite in one dimension (the direction of incidence) and infinite in the other dimension (normal to the direction of incidence). The history of individual electrons is followed in the usual condensed random-walk technique developed by Berger (ref. 7). In each condensed step, the multiple scattering by atoms is calculated by using Goudsmit-Saunderson theory (refs. 9 and 10). The individual scattering cross section used is that due to Mott (ref. 11) with screening effects as given by Molière (ref. 12). The multiple inelastic scattering effects are sampled from the Landau distribution (ref. 13), modified in the manner of Blunck and Leisegang (ref. 14). The secondary electrons – both photoelectrons and those resulting from inelastic collisions with the atoms – are included in the transport calculation. For reasons of the necessary manageability of the calculations, the following specific assumptions are made:

(1) The inelastic scattering probability is calculated by using the Möller approach (ref. 15) which disregards electron binding effects. However, this disregard is not expected to have any significant effect at high electron energies.

(2) The electron-positron differences in the energy loss, knock-on electron production, and multiple elastic scattering are ignored.

(3) The electrons are not allowed to deflect at the time of energetic bremsstrahlung production nor are they allowed to deflect at the time of fast delta-ray production. These deflections are included in an approximate manner in the multiple elastic scattering deflections.

(4) The energy of a secondary electron is not subtracted from the energy of the primary electron producing it; the energy loss of the primary electron is determined entirely by the Landau distribution (that is, no correlation between large primary loss and energetic secondary electrons is considered).

This program is the basis of ETRAN-15 code of reference 16 which was the basis of the theoretical calculations. The results of Monte Carlo calculations are summarized in the appendix.

COMPARISON BETWEEN THEORY AND THE EXPERIMENTAL RESULTS

Figure 7 shows a comparison between the experimental spectra and the theoretical electron energy histograms for a number of target thicknesses. Figure 8 shows a similar comparison after modifying the theoretical energy histograms for the finite resolving power of the detection system. In both of these figures, the peak intensities of the Monte Carlo distribution functions have been arbitrarily adjusted to match the experimental spectral peaks for the convenience of comparison. If, on the other hand, one compares the observed and the calculated functions on the basis of equal areas under them, as would be the case if the Monte Carlo and the experimental results agreed on the total number of transmitted electrons, the experimental peak intensity will be relatively lower than the calculated peak intensity. The errors on the experimental data points in these figures are standard deviations of the counts per channel. The errors on the Monte Carlo points are given by the standard deviation of the appropriate number of electrons per 45 keV energy interval for 10 000 electrons normally incident on the target. These counts ranged from 1396 (0.485-mm-thick target, 5° to 15° angular interval in the energy interval 2250 keV to 2295 keV) to 25 (2.91-mm-thick target, 70° to 80° angular interval in the energy interval 1305 keV to 1350 keV). Thus, the statistical fluctuations in the calculated spectra are very large in the case of thicker targets at higher angles of observation. From figures 7 and 8, it is apparent that the experimental spectra are slightly broader than the theoretical spectra and that the theoretical spectra peak at slightly higher energies than the experimental spectra. It is possible that part of this discrepancy could be due to incomplete elimination of the effects of the incident electron energy straggle and the angular spread from the experimental spectra. However, the dependence of the discrepancy on the target thickness and the angle of observation

suggests inadequacy of the Blunck-Leisegang correction to the Landau distribution. A more accurate incorporation of the energy straggling effects and the inclusion of the correlation effects ignored in the present calculations may lead to better agreement.[2] Figure 9 shows a comparison between the experimentally observed angular distribution and the theoretically predicted distribution for two different target thicknesses. The errors on the experimental angular distribution points range from about 1 percent in the forward direction in thin targets to about 5 percent in the near normal direction ($\theta = 85^{o}$) for thick targets. Corresponding errors on the Monte Carlo points are about a factor of 2 higher. (See table I.) The agreement between the theoretical values and the experimental data is quite good. The agreement is equally good for other target thicknesses. Figures 10 and 11 show a comparison of the Bethe function (ref. 21) with the experimental and the Monte Carlo angular distributions, respectively. It appears that the Bethe function is in reasonably good agreement with the experiment and the theory except in the forward direction. Figure 12 shows the dependence of average electron deflection (refs. 1 and 2) on the target thickness. The errors in $\langle\cos\theta\rangle_{exp}$ range from about 1 percent in the case of 0.485-mm-thick target to as high as 5 percent in the case of 2.91-mm-thick target. As with the angular distribution data, the Monte Carlo points have a slightly larger error. A least-square fit of the experimental data was obtained to an expression of the following form:

$$\langle\cos\theta\rangle_{exp} = a_0 + a_1 \exp\left[-\left(\frac{d_0 - t}{d_0}\right)^i\right]$$

where

a_0, a_1 constants

i integer

t target thickness

d_0 penetration depth at which $\langle\cos\theta\rangle$ becomes independent of target thickness $\left(\text{for } t \gtrsim d_0, \left(d_0 - t\right) \text{ is equated to zero}\right)$

For a value of $i = 3$, the least-square analysis, verified by a numerical χ^2 test, shows that after a target thickness of 2.5 ± 0.1 mm, the incident electron beam does not diffuse out any further. The asymptotic value of the experimental average cosine of deflection

[2]Nigam et al. (ref. 17) have shown that the Molière theory, which has been used in the present calculations, contains an incorrect approximation for obtaining the screening angle. (Scott (ref. 18), however, has shown that the Nigam et al. distribution contains its own errors.) The use of a generalization of Foldy-Watson equations (ref. 19) in evaluating elastic and inelastic electron scattering may predict results in better agreement with the experimental data. The essential feature of this generalization is a more accurate description of the atomic form factor as it enters small angle scattering cross section. Recently, Scalettar (ref. 20) has used this technique to obtain the solution of electron transport equations for aluminum targets of thickness comparable to the electron range with rather good results.

angle is estimated to be 0.745 ± 0.020. This value is in good agreement with the Monte Carlo value 0.740 ± 0.020 and the value obtained from the Bethe function (0.706). The assumption of an isotropic distribution gives $\langle \cos \theta \rangle = 2/3$.

From these comparisons, it appears that the theory in its present form correctly predicts the angular distribution, although it does not predict an equally good spectral distribution, of the transmitted electrons. The total number of transmitted electrons should also be correctly predicted by the theory in its present form since the potentially influential factors that were ignored in the theoretical calculations, namely, electron deflections in inelastic collisions and correlation effects in larger angle deflections, should equally affect the angular distribution functions. This conclusion is also supported by the data presented in references 7, 16, and 22. Under these circumstances, a function of the form:

$$R = 2\pi \int_0^{\pi/2} R(\theta) \sin \theta \, d\theta = 2\pi \int_0^{\pi/2} \int_0^{E} n(E, \theta) \, E \sin \theta \, dE \, d\theta$$

can be used to compare the measured and calculated values of the radiation field intensity (due to electrons only) behind an absorbing medium. In this equation, R represents the total energy content of the transmitted electrons and $n(E,\theta)$ stands for the number of electrons in the energy range, E and E + dE and angular range, θ and $\theta + d\theta$. The values of $\left(R(\theta)_{exp} - R(\theta)_{theor}\right)/R(\theta)_{exp}$ range from about 5 percent in the case of 0.485-mm-thick target at $\theta = 10^{o}$ to about 16 percent in the case of 2.910-mm-thick target at $\theta = 75^{o}$. (Part of this larger discrepancy could be of a statistical nature because only a small fraction of the incident electrons penetrate deeply.) The discrepancy between the calculated and theoretical values of the transmitted electron energy density thus appears to increase as the absorbing medium thickness increases and this increase indicates the importance of the factors neglected in the theoretical calculations.

CONCLUSIONS

From the measurements of the energy and angular distributions of electrons transmitted through silicon targets of various thicknesses and their comparison with the Monte Carlo results, the following conclusions are drawn:

1. The inclusion of energy straggling effects improves the agreement between the theory and the experiment. In previous reports, the experimental results have been compared with the theoretical calculations in the continuous slowing down approximation and with partial inclusion of energy loss straggling effects. The agreement then was considerably worse than in the present case. A more accurate incorporation of the straggling effects function and inclusion of the correlation effects ignored in the present calculation should lead to improved agreement between the theory and the experiment.

2. Notwithstanding the statements in the preceding paragraph, the agreement between the experiment and the Monte Carlo calculations is rather satisfactory for the cases considered. Even for a 50-percent target thickness, the discrepancy between the experimental and calculated values of transmitted electron energy density at $\theta = 85^{\circ}$ is no more than 20 percent. It would be desirable to compare the theory with the experiment for thicker targets and at higher electron energies. At higher electron energies, the radiative collisions play a more significant role and may necessitate a more detailed theory.

3. The target thickness at which the average cosine of scattering angles reaches its asymptotic value is measured to be 2.5 ± 0.1 mm for 2.43 MeV electrons normally incident on plane-parallel silicon targets. The value of $\langle \cos \theta \rangle_{\text{exp-asym}}$ is determined to be 0.745 ± 0.020 compared with $\langle \cos \theta \rangle = 2/3$ for isotropic distribution.

Langley Research Center,
National Aeronautics and Space Administration,
Langley Station, Hampton, Va., July 11, 1968,
124-09-11-04-23.

APPENDIX

METHOD OF CALCULATING TRANSMITTED ELECTRON SPECTRA AND ANGULAR DISTRIBUTIONS

The main problem is to solve an electron-photon cascade reaction in which one type of radiation acts as a source for the other type. The electron collisions are too numerous to be followed individually. Consequently, a scheme of condensed random walk, whose main purpose is to group a large number of collisions into a single step, is used to break up the entire electron track into a manageable number of steps. The step sizes were chosen to fulfill the requirements for the validity of Goudsmit-Saunderson theory which was used to calculate multiple scattering effects within a step. In the present calculations, the step size was chosen so that, on the average, the electron energy decreased by a factor of 2^{-8} per step. The energy-loss calculations in each step were made by use of the Landau distribution as modified by Blunck and Leisegang. The probability of knock-on electron production is calculated by use of the Möller cross section and the histories of these electrons are followed. The probability of bremsstrahlung production is calculated by using Bethe-Heitler theory and the histories of photon-produced electrons are followed. The specific calculations are now described.

Ten thousand normally incident electrons, of energy 2.43 MeV, are followed in plane-parallel silicon targets with the following boundaries:

Boundaries	Fraction of CSDA range
0 and 0.485 mm	0.07839
0 and 0.970 mm	.15678
0 and 1.455 mm	.23517
0 and 2.425 mm	.39195
0 and 2.910 mm	.47034

The continuous slowing down approximation (CSDA) range for 2.43 MeV electrons in silicon was taken to be 1.442 g/cm^2. The boundary dimensions normal to the direction of incidence are assumed to be infinite. (Even though the target dimension in this direction is only 1 centimeter, this value may not be expected to introduce any error because most of the electrons will be stopped before escaping from the target sides.) The following effects are included in the calculations in order to obtain the relevant information:

(1) Straggling effects in electron collision and radiation energy loss are included in the energy loss by the electrons

(2) Knock-on secondary electron production is followed and its subsequent contributions are included

(3) No coupled inelastic deflection is permitted

(4) Bremsstrahlung and characteristic X-ray quanta production is followed and their effects on electron population are included

(5) The electrons – primary and secondary – are followed until their kinetic energy has fallen down to 225 KeV.

The Monte Carlo analysis is carried out for eighteen 5^{o} angular increments. Each Monte Carlo histogram is divided into 45 keV wide energy intervals. The calculated results are summarized in tables I to III.

REFERENCES

1. Singh, Jag J.: Transmission of Electrons Through Thin Silicon Foils. Bull. Amer. Phys. Soc., ser. II, vol. 10, no. 1, 1965, p. 68.

2. Singh, Jag J.: Electron Transmission Through Thick Silicon Targets. NASA TN D-3927, 1967.

3. Rester, David H.; and Rainwater, Walter J., Jr.: Part 2. Electron Scattering in Aluminum. Investigations of Electron Interactions With Matter, NASA CR-334, 1965, pp. 45-90.

4. Rester, David H.; and Rainwater, Walter J., Jr.: Measurement of the Transmission Spectra of 1-MeV Electrons With Normal Incidence on Aluminum Slabs. J. Appl. Phys., vol. 37, no. 4, Mar. 15, 1966, pp. 1793-1797.

5. Jupiter, C. P.; Lonergan, J. A.; and Merkel, G.: An Experimental Study of the Transport of Electrons Through Thick Targets. Trans. Amer. Nucl. Soc., vol. 10, no. 1, June 1967, pp. 378-379.

6. Frank, H.: Multiple Scattering and Back-Diffusion of Fast Electrons After Passage Through Thick Layers. Z. Naturforsch., vol. 14a, 1959, pp. 247-261.

7. Berger, Martin J.: Monte Carlo Calculation of the Penetration and Diffusion of Fast Charged Particles. Methods in Computational Physics, Vol. 1 – Statistical Physics, Berni Alder, Sidney Fernbach, and Manuel Rotenberg, eds., Academic Press, 1963, pp. 135-215.

8. Aero-Space Div., Boeing Co.: Computer Codes for Space Radiation Environment and Shielding. WL TDR-64-71, vol. I, U.S. Air Force, Aug. 1964.

9. Goudsmit, S.; and Saunderson, J. L.: Multiple Scattering of Electrons. Phys. Rev., Second ser., vol. 57, no. 1, Jan. 1, 1940, pp. 24-29.

10. Goudsmit, S.; and Saunderson, J. L.: Multiple Scattering of Electrons. II. Phys. Rev., Second ser., vol. 58, no. 1, July 1, 1940, pp. 36-42.

11. Mott, N. F.: The Scattering of Fast Electrons by Atomic Nuclei. Proc. Roy. Soc. (London), ser. A, vol. 124, 1929, pp. 425-442.

12. Molière, Gert: Theory of Scattering of Fast Charged Particles. Part I. Single Scattering by the Shielded Coulomb Field. Transl. 19G5G, Ass. Tech. Serv., [Mar. 1955].

13. Landau, L.: Energy Loss of Fast Particles by Ionization. J. Phys. (U.S.S.R.), vol. 8, 1944, pp. 201-205.

14. Blunck, O.; and Leisegang, S.: Energy Loss of Fast Electrons in Thin Layers. Z. Physik, vol. 128, 1950, pp. 500-505.

15. Möller, C.: Passage of Hard β-Rays Through Matter. Ann. Physik, vol. 14, no. 5, Aug. 15, 1932, pp. 531-585.

16. Berger, Martin J.; and Seltzer, Stephen M.: Penetration of Electrons and Associated Bremsstrahlung Through Aluminum Shields. Trans. Amer. Nucl. Soc., vol. 10, no. 1, June 1967, pp. 379-380.

17. Nigam, B. P.; Sundaresan, M. K.; and Wu, Ta-You: Theory of Multiple Scattering: Second Born Approximation and Corrections to Molière's Work. Phys. Rev., vol. 115, no. 3, Aug. 1959, pp. 491-502.

18. Scott, William T.: The Theory of Small-Angle Multiple Scattering of Fast Charged Particles. Rev. Modern Phys., vol. 35, no. 2, Apr. 1963, pp. 231-313.

19. Watson, Kenneth M.: Quantum Mechanical Transport Theory. I. Incoherent Processes. Phys. Rev., vol. 118, no. 4, May 15, 1960, pp. 886-898.

20. Scalettar, Richard: The Theory of the Transport of Relativistic Electrons. Trans. Amer. Nucl. Soc., vol. 10, no. 1, June 1967, p. 380.

21. Bethe, H. A.; Rose, M. E.; and Smith, L. P.: Multiple Scattering of Electrons. Proc. Amer. Phil. Soc., vol. 78, 1938, pp. 573-585.

22. Hardy, Alva C.; Lopez, Manuel D.; and White, Timothy T.: A Parametric Technique of Computing Primary Electron Dose. Trans. Amer. Nucl. Soc., vol. 10, no. 1, June 1967, p. 383.

TABLE I.- ANGULAR DISTRIBUTION OF TRANSMITTED ELECTRONS

Angular range		Number of electrons/sr normalized to one incident electron				
θ_1, deg	θ_2, deg	0.113 g/cm^2 or 0.485 mm	0.226 g/cm^2 or 0.970 mm	0.339 g/cm^2 or 1.455 mm	0.565 g/cm^2 or 2.425 mm	0.678 g/cm^2 or 2.910 mm
0	5	1.79	8.91×10^{-1}	6.36×10^{-1}	3.26×10^{-1}	2.89×10^{-1}
5	10	1.76	8.87×10^{-1}	5.80×10^{-1}	3.51×10^{-1}	2.64×10^{-1}
10	15	1.35	7.86×10^{-1}	5.18×10^{-1}	3.01×10^{-1}	2.69×10^{-1}
15	20	1.05	6.61×10^{-1}	5.14×10^{-1}	2.98×10^{-1}	2.21×10^{-1}
20	25	7.30×10^{-1}	5.48×10^{-1}	4.26×10^{-1}	2.76×10^{-1}	2.07×10^{-1}
25	30	4.56×10^{-1}	4.61×10^{-1}	3.75×10^{-1}	2.62×10^{-1}	1.94×10^{-1}
30	35	2.92×10^{-1}	3.74×10^{-1}	3.00×10^{-1}	2.38×10^{-1}	1.73×10^{-1}
35	40	1.74×10^{-1}	2.63×10^{-1}	2.83×10^{-1}	1.97×10^{-1}	1.61×10^{-1}
40	45	9.34×10^{-2}	1.88×10^{-1}	2.07×10^{-1}	1.69×10^{-1}	1.31×10^{-1}
45	50	5.30×10^{-2}	1.39×10^{-1}	1.68×10^{-1}	1.38×10^{-1}	1.10×10^{-1}
50	55	2.67×10^{-2}	1.02×10^{-1}	1.36×10^{-1}	1.25×10^{-1}	9.82×10^{-2}
55	60	2.10×10^{-2}	7.59×10^{-2}	9.91×10^{-2}	9.41×10^{-2}	7.89×10^{-2}
60	65	1.21×10^{-2}	5.59×10^{-2}	8.51×10^{-2}	7.30×10^{-2}	5.37×10^{-2}
65	70	7.50×10^{-3}	3.59×10^{-2}	5.90×10^{-2}	4.34×10^{-2}	4.34×10^{-2}
70	75	4.97×10^{-3}	2.47×10^{-2}	4.13×10^{-2}	4.48×10^{-2}	3.23×10^{-2}
75	80	3.55×10^{-3}	1.46×10^{-2}	2.47×10^{-2}	2.54×10^{-2}	2.07×10^{-2}
80	85	7.36×10^{-4}	7.91×10^{-3}	1.71×10^{-2}	1.53×10^{-2}	1.27×10^{-2}
85	90	7.30×10^{-4}	4.20×10^{-3}	7.30×10^{-3}	7.67×10^{-3}	6.76×10^{-3}

TABLE II.- ANGULAR DISTRIBUTION OF REFLECTED ELECTRONS

Angular interval		Number of electrons/sr normalized to one incident electron				
$\theta 1$, deg	$\theta 2$, deg	0.113 g/cm^2	0.226 g/cm^2	0.339 g/cm^2	0.565 g/cm^2	0.678 g/cm^2
0	5	0.0	4.18×10^{-3}	1.25×10^{-2}	1.67×10^{-2}	1.67×10^{-2}
5	10	1.40×10^{-3}	4.19×10^{-3}	1.54×10^{-2}	2.52×10^{-2}	2.52×10^{-2}
10	15	0.0	3.37×10^{-3}	1.52×10^{-2}	2.36×10^{-2}	2.36×10^{-2}
15	20	6.07×10^{-4}	4.25×10^{-3}	1.21×10^{-2}	1.88×10^{-2}	1.94×10^{-2}
20	25	4.77×10^{-4}	2.86×10^{-3}	1.48×10^{-2}	1.95×10^{-2}	1.95×10^{-2}
25	30	1.19×10^{-3}	5.93×10^{-3}	1.26×10^{-2}	1.94×10^{-2}	1.94×10^{-2}
30	35	1.02×10^{-3}	4.75×10^{-3}	1.29×10^{-2}	1.94×10^{-2}	1.94×10^{-2}
35	40	1.80×10^{-3}	7.19×10^{-3}	1.29×10^{-2}	1.86×10^{-2}	1.86×10^{-2}
40	45	5.40×10^{-4}	4.05×10^{-3}	1.05×10^{-2}	1.35×10^{-2}	1.35×10^{-2}
45	50	4.95×10^{-4}	2.72×10^{-3}	9.16×10^{-3}	1.29×10^{-2}	1.29×10^{-2}
50	55	6.90×10^{-4}	3.22×10^{-3}	5.98×10^{-3}	9.89×10^{-3}	9.89×10^{-3}
55	60	1.51×10^{-3}	4.11×10^{-3}	6.92×10^{-3}	9.52×10^{-3}	9.52×10^{-3}
60	65	1.44×10^{-3}	4.73×10^{-3}	6.79×10^{-3}	8.02×10^{-3}	8.02×10^{-3}
65	70	1.18×10^{-3}	1.97×10^{-3}	4.74×10^{-3}	5.53×10^{-3}	5.53×10^{-3}
70	75	3.83×10^{-4}	1.91×10^{-3}	4.21×10^{-3}	5.16×10^{-3}	5.16×10^{-3}
75	80	3.74×10^{-4}	7.47×10^{-4}	1.68×10^{-3}	2.06×10^{-3}	2.06×10^{-3}
80	85	3.68×10^{-4}	7.36×10^{-4}	1.10×10^{-3}	1.66×10^{-3}	1.66×10^{-3}
85	90	1.83×10^{-4}	7.30×10^{-4}	9.13×10^{-4}	1.66×10^{-3}	1.64×10^{-3}

TABLE III.- ENERGY SPECTRA AND ANGULAR DISTRIBUTION OF ELECTRONS TRANSMITTED THROUGH SILICON SLABS OF VARIOUS THICKNESSES

[The transmitted electron intensities are expressed in units of Number/MeV-sr normalized to one incident particle]

(a) Target thickness = 0.07839 CSDA range = 0.1130 g/cm^2

Energy, E, MeV	Angular distributions for θ, deg, of –									
	0 to 5.000	5.000 to 10.000	10.000 to 15.000	15.000 to 20.000	20.000 to 25.000	25.000 to 30.000	30.000 to 35.000	35.000 to 40.000	40.000 to 45.000	45.000 to 50.000
2.4300 to 2.3850	0.0	0.0	0.0	0.0	0.0	0.0	0.0	0.0	0.0	0.0
2.3850 to 2.3400	0.0	0.0	1.87E-02	0.0	0.0	8.78E-03	0.0	0.0	0.0	0.0
2.3400 to 2.2950	1.06E 01	1.00E 01	8.60E 00	6.50E 00	4.07E 00	2.19E 00	1.27E 00	6.66E-01	2.94E-01	1.43E-01
2.2950 to 2.2500	2.04E 01	1.95E 01	1.43E 01	1.13E 01	8.21E 00	4.98E 00	3.12E 00	2.02E 00	1.09E 00	5.50E-01
2.2500 to 2.2050	3.90E 00	4.81E 00	3.41E 00	2.59E 00	1.80E 00	1.33E 00	9.96E-01	6.06E-01	3.24E-01	2.14E-01
2.2050 to 2.1600	1.86E 00	2.08E 00	1.39E 00	9.57E-01	7.20E-01	5.88E-01	3.92E-01	1.73E-01	1.14E-01	8.80E-02
2.1600 to 2.1150	4.65E-01	8.39E-01	7.31E-01	6.88E-01	4.45E-01	2.46E-01	2.49E-01	7.33E-02	7.20E-02	2.75E-02
2.1150 to 2.0700	9.29E-01	2.80E-01	4.50E-01	2.56E-01	2.75E-01	1.93E-01	6.04E-02	7.33E-02	1.20E-02	1.10E-02
2.0700 to 2.0250	1.86E-01	3.42E-01	3.93E-01	1.75E-01	1.70E-01	1.05E-01	4.53E-02	4.00E-02	2.40E-02	2.20E-02
2.0250 to 1.9800	3.72E-01	3.42E-01	2.06E-01	2.16E-01	8.48E-02	7.90E-02	3.02E-02	2.00E-02	3.00E-02	1.10E-02
1.9800 to 1.9350	9.29E-02	2.17E-01	1.50E-01	1.75E-01	6.36E-02	7.90E-02	4.53E-02	2.66E-02	1.80E-02	1.65E-02
1.9350 to 1.8900	9.29E-02	1.55E-01	1.31E-01	9.44E-02	6.36E-02	5.27E-02	4.53E-02	1.33E-02	1.20E-02	0.0
1.8900 to 1.8450	1.86E-01	6.21E-02	1.87E-02	4.04E-02	5.30E-02	4.39E-02	5.28E-02	1.33E-02	0.0	0.0
1.8450 to 1.8000	1.86E-01	6.21E-02	1.87E-02	4.04E-02	0.0	1.76E-02	1.51E-02	6.66E-03	0.0	5.50E-03
1.8000 to 1.7550	9.29E-02	6.21E-02	0.0	1.35E-02	4.24E-02	8.78E-03	0.0	6.66E-03	1.20E-02	0.0
1.7550 to 1.7100	9.29E-02	6.21E-02	3.75E-02	5.39E-02	1.06E-02	8.78E-03	7.55E-03	6.66E-03	0.0	0.0
1.7100 to 1.6650	0.0	9.32E-02	1.87E-02	1.35E-02	2.12E-02	0.0	1.51E-02	6.66E-03	0.0	0.0
1.6650 to 1.6200	0.0	0.0	1.87E-02	4.04E-02	2.12E-02	1.76E-02	0.0	6.66E-03	0.0	0.0
1.6200 to 1.5750	0.0	0.0	0.0	1.35E-02	1.06E-02	0.0	1.51E-02	6.66E-03	0.0	0.0
1.5750 to 1.5300	0.0	3.11E-02	1.87E-02	1.35E-02	1.06E-02	0.0	1.51E-02	0.0	0.0	0.0
1.5300 to 1.4850	9.29E-02	3.11E-02	1.87E-02	2.70E-02	1.06E-02	2.63E-02	0.0	0.0	0.0	0.0
1.4850 to 1.4400	0.0	0.0	0.0	4.04E-02	0.0	1.76E-02	7.55E-03	6.66E-03	6.00E-03	0.0
1.4400 to 1.3950	1.86E-01	3.11E-02	0.0	4.04E-02	0.0	0.0	0.0	0.0	0.0	0.0
1.3950 to 1.3500	0.0	3.11E-02	0.0	0.0	0.0	0.0	0.0	0.0	0.0	5.50E-03
1.3500 to 1.3050	0.0	0.0	1.87E-02	0.0	0.0	0.0	0.0	0.0	0.0	0.0
1.3050 to 1.2600	0.0	0.0	0.0	0.0	0.0	8.78E-03	0.0	0.0	0.0	0.0
1.2600 to 1.2150	0.0	0.0	1.87E-02	0.0	1.06E-02	0.0	7.55E-03	0.0	0.0	0.0
1.2150 to 1.1700	0.0	0.0	0.0	0.0	0.0	0.0	0.0	0.0	0.0	0.0
1.1700 to 1.1250	0.0	0.0	0.0	0.0	0.0	0.0	0.0	6.66E-03	0.0	0.0
1.1250 to 1.0800	0.0	0.0	0.0	0.0	0.0	0.0	0.0	6.66E-03	6.00E-03	0.0
1.0800 to 1.0350	0.0	3.11E-02	0.0	0.0	0.0	8.78E-03	0.0	0.0	6.00E-03	0.0
1.0350 to 0.9900	0.0	0.0	0.0	2.70E-02	1.06E-02	0.0	0.0	0.0	6.00E-03	0.0
0.9900 to 0.9450	0.0	0.0	1.87E-02	0.0	0.0	0.0	0.0	6.66E-03	0.0	0.0
0.9450 to 0.9000	0.0	0.0	0.0	0.0	2.12E-02	1.76E-02	0.0	6.66E-03	0.0	5.50E-03
0.9000 to 0.8550	0.0	0.0	0.0	1.35E-02	0.0	8.78E-03	0.0	6.66E-03	0.0	0.0
0.8500 to 0.8100	0.0	0.0	0.0	0.0	1.06E-02	0.0	2.26E-02	0.0	0.0	1.10E-02
0.8100 to 0.7650	0.0	0.0	0.0	0.0	1.06E-02	8.78E-03	0.0	6.66E-03	1.20E-02	0.0
0.7650 to 0.7200	0.0	0.0	1.87E-02	0.0	1.06E-02	0.0	7.55E-03	0.0	0.0	0.0
0.7200 to 0.6750	0.0	0.0	0.0	0.0	0.0	1.76E-02	1.51E-02	6.66E-03	0.0	0.0
0.6750 to 0.6300	0.0	0.0	0.0	0.0	0.0	1.76E-02	0.0	0.0	0.0	0.0
0.6300 to 0.5850	0.0	3.11E-02	1.87E-02	0.0	0.0	0.0	7.55E-03	1.33E-02	0.0	0.0
0.5850 to 0.5400	9.29E-02	6.21E-02	0.0	1.35E-02	2.12E-02	0.0	7.55E-03	6.66E-03	1.20E-02	5.50E-03
0.5400 to 0.4950	0.0	0.0	0.0	0.0	0.0	0.0	0.0	6.66E-03	0.0	0.0
0.4950 to 0.4500	0.0	3.11E-02	0.0	5.39E-02	2.12E-02	1.76E-02	1.51E-02	0.0	0.0	5.50E-03
0.4500 to 0.4050	0.0	0.0	0.0	0.0	0.0	0.0	7.55E-03	1.33E-02	6.00E-03	5.50E-03
0.4050 to 0.3600	0.0	0.0	0.0	0.0	0.0	1.76E-02	7.55E-03	1.33E-02	0.0	1.65E-02
0.3600 to 0.3150	9.29E-02	0.0	1.87E-02	1.35E-02	1.06E-02	0.0	1.51E-02	0.0	0.0	1.10E-02
0.3150 to 0.2700	0.0	0.0	0.0	0.0	1.06E-02	8.78E-03	0.0	6.66E-03	1.20E-02	1.65E-02
0.2700 to 0.2250	0.0	3.11E-02	0.0	0.0	0.0	1.76E-02	0.0	0.0	6.00E-03	5.50E-03

TABLE III.- ENERGY SPECTRA AND ANGULAR DISTRIBUTION OF ELECTRONS TRANSMITTED THROUGH SILICON SLABS OF VARIOUS THICKNESSES – Continued

(a) Target thickness = 0.07839 CSDA range = 0.1130 g/cm^2 – Concluded

Energy, E, MeV	Angular distributions for θ, deg, of –							
	50.000 to 55.000	55.000 to 60.000	60.000 to 65.000	65.000 to 70.000	70.000 to 75.000	75.000 to 80.000	80.000 to 85.000	85.000 to 90.000
2.4300 to 2.3850	0.0	0.0	0.0	0.0	0.0	0.0	0.0	0.0
2.3850 to 2.3400	0.0	0.0	0.0	0.0	0.0	0.0	0.0	0.0
2.3400 to 2.2950	3.07E-02	2.88E-02	4.57E-03	0.0	0.0	0.0	0.0	0.0
2.2950 to 2.2500	2.15E-01	1.39E-01	9.14E-02	3.51E-02	4.25E-03	0.0	0.0	0.0
2.2500 to 2.2050	1.69E-01	1.39E-01	6.86E-02	3.51E-02	3.40E-02	1.25E-02	4.09E-03	0.0
2.2050 to 2.1600	3.58E-02	3.85E-02	2.74E-02	1.32E-02	1.70E-02	2.08E-02	0.0	0.0
2.1600 to 2.1150	1.53E-02	1.44E-02	1.83E-02	2.19E-02	0.0	0.0	0.0	4.06E-03
2.1150 to 2.0700	5.11E-03	1.44E-02	0.0	2.19E-02	4.25E-03	8.31E-03	0.0	0.0
2.0700 to 2.0250	5.11E-03	4.81E-03	9.14E-03	1.32E-02	1.28E-02	0.0	4.09E-03	0.0
2.0250 to 1.9800	1.02E-02	1.44E-03	4.57E-03	0.0	4.25E-03	4.15E-03	0.0	4.06E-03
1.9800 to 1.9350	0.0	1.44E-02	4.57E-03	1.32E-03	4.25E-03	0.0	0.0	0.0
1.9350 to 1.8900	1.02E-02	4.81E-03	0.0	0.0	0.0	4.15E-03	0.0	0.0
1.8900 to 1.8450	1.53E-02	0.0	0.0	0.0	0.0	0.0	0.0	0.0
1.8450 to 1.8000	5.11E-03	0.0	4.57E-03	0.0	0.0	0.0	0.0	0.0
1.8000 to 1.7550	0.0	0.0	0.0	0.0	0.0	4.15E-03	0.0	0.0
1.7550 to 1.7100	0.0	4.81E-03	0.0	0.0	0.0	0.0	0.0	0.0
1.7100 to 1.6650	0.0	4.81E-03	0.0	0.0	4.25E-03	0.0	4.09E-03	0.0
1.6650 to 1.6200	0.0	0.0	0.0	0.0	0.0	0.0	0.0	0.0
1.6200 to 1.5750	1.02E-02	0.0	0.0	0.0	0.0	0.0	0.0	0.0
1.5750 to 1.5300	5.11E-03	0.0	4.57E-03	0.0	0.0	4.15E-03	0.0	0.0
1.5300 to 1.4850	1.02E-02	0.0	0.0	0.0	0.0	0.0	0.0	0.0
1.4850 to 1.4400	0.0	0.0	0.0	0.0	0.0	0.0	0.0	0.0
1.4400 to 1.3950	0.0	0.0	0.0	0.0	0.0	0.0	0.0	0.0
1.3950 to 1.3500	0.0	0.0	0.0	0.0	0.0	0.0	0.0	0.0
1.3500 to 1.3050	0.0	0.0	4.57E-03	0.0	0.0	0.0	4.09E-03	0.0
1.3050 to 1.2600	0.0	0.0	0.0	0.0	0.0	0.0	0.0	0.0
1.2600 to 1.2150	0.0	0.0	0.0	0.0	0.0	0.0	0.0	0.0
1.2150 to 1.1700	0.0	0.0	0.0	0.0	0.0	0.0	0.0	0.0
1.1700 to 1.1250	0.0	0.0	0.0	0.0	0.0	0.0	0.0	0.0
1.1250 to 1.0800	0.0	4.81E-03	4.57E-03	0.0	0.0	0.0	0.0	0.0
1.0800 to 1.0350	0.0	0.0	0.0	0.0	0.0	0.0	0.0	0.0
1.0350 to 0.9900	0.0	4.81E-03	0.0	0.0	0.0	0.0	0.0	0.0
0.9900 to 0.9450	0.0	0.0	0.0	0.0	0.0	4.15E-03	0.0	0.0
0.9450 to 0.9000	1.02E-02	0.0	0.0	0.0	4.25E-03	0.0	0.0	0.0
0.9000 to 0.8550	0.0	0.0	0.0	0.0	0.0	0.0	0.0	0.0
0.8550 to 0.8100	0.0	0.0	0.0	0.0	4.25E-03	0.0	0.0	0.0
0.8100 to 0.7650	5.11E-03	0.0	0.0	0.0	0.0	0.0	0.0	0.0
0.7650 to 0.7200	5.11E-03	4.81E-03	0.0	0.0	0.0	4.15E-03	0.0	0.0
0.7200 to 0.6750	0.0	0.0	0.0	0.0	0.0	0.0	0.0	0.0
0.6750 to 0.6300	0.0	4.81E-03	0.0	0.0	0.0	4.15E-03	0.0	0.0
0.6300 to 0.5850	0.0	0.0	0.0	0.0	0.0	0.0	0.0	0.0
0.5850 to 0.5400	1.02E-02	4.81E-03	4.57E-03	4.39E-03	0.0	4.15E-03	0.0	0.0
0.5400 to 0.4950	5.11E-03	0.0	9.14E-03	0.0	0.0	0.0	0.0	4.06E-03
0.4950 to 0.4500	5.11E-03	4.81E-03	0.0	0.0	0.0	0.0	0.0	0.0
0.4500 to 0.4050	0.0	0.0	0.0	0.0	0.0	0.0	0.0	0.0
0.4050 to 0.3600	0.0	0.0	0.0	0.0	0.0	0.0	0.0	4.06E-03
0.3600 to 0.3150	0.0	4.81E-03	0.0	0.0	0.0	0.0	0.0	0.0
0.3150 to 0.2700	0.0	0.0	4.57E-03	4.39E-03	1.28E-02	4.15E-03	0.0	0.0
0.2700 to 0.2250	1.02E-02	9.61E-03	4.57E-03	4.39E-03	4.25E-03	0.0	0.0	0.0

TABLE III.- ENERGY SPECTRA AND ANGULAR DISTRIBUTION OF ELECTRONS TRANSMITTED THROUGH SILICON SLABS OF VARIOUS THICKNESSES – Continued

(b) Target thickness = 0.15678 CSDA range = 0.2260 g/cm^2

Energy, E, Mev	Angular distributions for θ, deg, of –									
	0.0 to 5.000	5.000 to 10.000	10.000 to 15.000	15.000 to 20.000	20.000 to 25.000	25.000 to 30.000	30.000 to 35.000	35.000 to 40.000	40.000 to 45.000	45.000 to 50.000
2.4300 to 2.3850	0.0	0.0	0.0	0.0	0.0	0.0	0.0	0.0	0.0	0.0
2.3850 to 2.3400	0.0	0.0	0.0	0.0	0.0	0.0	0.0	0.0	0.0	0.0
2.3400 to 2.2950	0.0	0.0	0.0	0.0	0.0	0.0	0.0	0.0	0.0	0.0
2.2950 to 2.2500	0.0	0.0	0.0	0.0	0.0	0.0	0.0	0.0	0.0	0.0
2.2500 to 2.2050	0.0	0.0	3.75E-02	1.35E-02	2.12E-02	0.0	1.51E-02	0.0	0.0	0.0
2.2050 to 2.1600	2.32E 00	2.39E 00	2.15E 00	1.62E 00	1.21E 00	8.25E-01	5.51E-01	3.20E-01	1.80E-01	7.70E-02
2.1600 to 2.1150	7.53E 00	6.80E 00	5.99E 00	5.06E 00	3.95E 00	3.10E 00	2.48E 00	1.59E 00	1.06E 00	6.10E-01
2.1150 to 2.0700	3.44E 00	4.69E 00	3.90E 00	3.51E 00	2.69E 00	2.47E 00	2.07E 00	1.64E 00	1.13E 00	8.85E-01
2.0700 to 2.0250	2.32E 00	2.52E 00	1.85E 00	1.46E 00	1.57E 00	1.28E 00	1.19E 00	7.33E-01	6.76E-01	4.62E-01
2.0250 to 1.9800	1.39E 00	8.39E-01	1.12E 00	6.88E-01	8.69E-01	7.38E-01	5.43E-01	4.13E-01	2.88E-01	3.52E-01
1.9800 to 1.9350	5.58E-01	4.35E-01	5.81E-01	5.66E-01	4.56E-01	4.30E-01	2.72E-01	2.86E-01	1.80E-01	1.81E-01
1.9350 to 1.8900	3.72E-01	6.52E-01	3.93E-01	2.70E-01	2.75E-01	2.72E-01	2.72E-01	1.40E-01	1.38E-01	4.40E-02
1.8900 to 1.8450	4.65E-01	3.11E-01	2.62E-01	3.51E-01	1.59E-01	2.02E-01	1.51E-01	1.13E-01	4.80E-02	6.60E-02
1.8450 to 1.8000	3.72E-01	2.17E-01	2.06E-01	3.24E-01	1.80E-01	1.76E-01	1.13E-01	1.60E-01	4.20E-02	6.60E-02
1.8000 to 1.7550	1.86E-01	1.86E-01	1.69E-01	9.44E-02	1.59E-01	1.49E-01	1.13E-01	6.66E-02	4.80E-02	4.95E-02
1.7550 to 1.7100	9.29E-02	1.24E-01	5.62E-02	1.48E-01	9.53E-02	1.05E-01	7.55E-02	5.99E-02	2.40E-02	3.30E-02
1.7100 to 1.6650	0.0	9.32E-02	1.31E-01	9.44E-02	5.30E-02	5.27E-02	6.04E-02	2.66E-02	5.40E-02	2.75E-02
1.6650 to 1.6200	9.29E-02	3.11E-02	1.87E-02	5.39E-02	4.24E-02	2.63E-02	3.02E-02	4.00E-02	3.60E-02	2.20E-02
1.6200 to 1.5750	9.29E-02	3.11E-02	3.75E-02	1.35E-02	4.24E-02	2.63E-02	2.26E-02	3.33E-02	3.60E-02	2.20E-02
1.5750 to 1.5300	9.29E-02	3.11E-02	3.75E-02	6.74E-02	2.12E-02	0.0	3.02E-02	2.00E-02	1.80E-02	0.0
1.5300 to 1.4850	0.0	0.0	3.75E-02	2.70E-02	3.18E-02	4.39E-02	3.02E-02	2.00E-02	1.80E-02	2.20E-02
1.4850 to 1.4400	9.29E-02	6.21E-02	0.0	4.04E-02	2.12E-02	2.63E-02	2.26E-02	0.0	6.00E-03	2.20E-02
1.4400 to 1.3950	9.29E-02	3.11E-02	3.75E-02	2.70E-02	0.0	1.76E-02	1.51E-02	2.66E-02	6.00E-03	1.10E-02
1.3950 to 1.3500	0.0	3.11E-02	0.0	1.35E-02	0.0	3.51E-02	3.02E-02	6.66E-03	6.00E-03	2.20E-02
1.3500 to 1.3050	9.29E-02	3.11E-02	3.75E-02	1.35E-02	2.12E-02	8.78E-03	0.0	0.0	3.00E-02	1.10E-02
1.3050 to 1.2600	0.0	0.0	1.87E-02	1.35E-02	0.0	8.78E-03	0.0	1.33E-02	1.80E-02	0.0
1.2600 to 1.2150	0.0	0.0	1.87E-02	2.70E-02	0.0	1.76E-02	7.55E-03	6.66E-03	6.00E-03	5.50E-03
1.2150 to 1.1700	0.0	0.0	1.87E-02	2.70E-02	3.18E-02	1.76E-02	7.55E-03	0.0	6.00E-03	0.0
1.1700 to 1.1250	0.0	0.0	5.62E-02	0.0	2.12E-02	1.76E-02	0.0	6.66E-03	0.0	5.50E-03
1.1250 to 1.0800	0.0	0.0	1.87E-02	0.0	1.06E-02	8.78E-03	7.55E-03	0.0	1.20E-02	5.50E-03
1.0800 to 1.0350	0.0	0.0	3.75E-02	1.35E-02	0.0	1.76E-02	7.55E-03	1.33E-02	0.0	0.0
1.0350 to 0.9900	0.0	0.0	0.0	1.35E-02	0.0	8.78E-03	2.26E-02	6.66E-03	0.0	0.0
0.9900 to 0.9450	0.0	0.0	0.0	0.0	2.12E-02	8.78E-03	7.55E-03	6.66E-03	0.0	0.0
0.9450 to 0.9000	0.0	0.0	1.87E-02	2.70E-02	2.12E-02	8.78E-03	0.0	0.0	1.20E-02	0.0
0.9000 to 0.8550	0.0	0.0	0.0	0.0	1.06E-02	8.78E-03	0.0	0.0	6.00E-03	5.50E-03
0.8550 to 0.8100	0.0	0.0	1.87E-02	0.0	0.0	8.78E-03	0.0	1.33E-02	6.00E-03	0.0
0.8100 to 0.7650	9.29E-02	3.11E-02	0.0	0.0	2.12E-02	1.76E-02	1.51E-02	1.33E-02	6.00E-03	0.0
0.7650 to 0.7200	0.0	0.0	1.87E-02	2.70E-02	0.0	0.0	1.51E-02	6.66E-03	0.0	0.0
0.7200 to 0.6750	0.0	0.0	3.75E-02	1.35E-02	2.12E-02	0.0	7.55E-03	0.0	1.20E-02	5.50E-03
0.6750 to 0.6300	0.0	6.21E-02	1.87E-02	2.70E-02	2.12E-02	8.78E-03	7.55E-03	0.0	0.0	5.50E-03
0.6300 to 0.5850	0.0	0.0	0.0	0.0	3.18E-02	0.0	0.0	1.33E-02	6.00E-03	5.50E-03
0.5850 to 0.5400	0.0	0.0	1.87E-02	1.35E-02	0.0	8.78E-03	1.51E-02	0.0	0.0	0.0
0.5400 to 0.4950	0.0	0.0	1.87E-02	0.0	2.12E-02	8.78E-03	7.55E-03	1.33E-02	6.00E-03	5.50E-03
0.4950 to 0.4500	0.0	3.11E-02	3.75E-02	1.35E-02	1.06E-02	8.78E-03	7.55E-03	2.00E-02	1.20E-02	1.10E-02
0.4500 to 0.4050	0.0	0.0	0.0	0.0	2.12E-02	1.76E-02	0.0	0.0	6.00E-03	5.50E-03
0.4050 to 0.3600	0.0	9.32E-02	3.75E-02	1.35E-02	1.06E-02	1.76E-02	1.51E-02	1.33E-02	0.0	1.10E-02
0.3600 to 0.3150	0.0	0.0	0.0	1.35E-02	2.12E-02	8.78E-03	1.51E-02	0.0	6.00E-03	5.50E-03
0.3150 to 0.2700	9.29E-02	0.0	1.87E-02	1.35E-02	1.06E-02	2.63E-02	3.02E-02	6.66E-03	1.80E-02	5.50E-03
0.2700 to 0.2250	0.0	0.0	0.0	0.0	0.0	8.78E-03	1.51E-02	6.66E-03	2.40E-02	1.10E-02

TABLE III.- *ENERGY SPECTRA AND ANGULAR DISTRIBUTION OF ELECTRONS TRANSMITTED* THROUGH SILICON SLABS OF VARIOUS THICKNESSES – Continued

(b) Target thickness = 0.15678 CSDA range = 0.2260 g/cm^2 – Concluded

Energy, E, Mev	Angular distributions for θ, deg, of –							
	50.000 to 55.000	55.000 to 60.000	60.000 to 65.000	65.000 to 70.000	70.000 to 75.000	75.000 to 80.000	80.000 to 85.000	85.000 to 90.000
2.4300 to 2.3850	0.0	0.0	0.0	0.0	0.0	0.0	0.0	0.0
2.3850 to 2.3400	0.0	0.0	0.0	0.0	0.0	0.0	0.0	0.0
2.3400 to 2.2950	0.0	0.0	0.0	0.0	0.0	0.0	0.0	0.0
2.2950 to 2.2500	0.0	0.0	0.0	0.0	0.0	0.0	0.0	0.0
2.2500 to 2.2050	0.0	0.0	0.0	0.0	0.0	0.0	0.0	0.0
2.2050 to 2.1600	4.09E-02	4.81E-03	0.0	0.0	0.0	0.0	0.0	0.0
2.1600 to 2.1150	3.17E-01	2.16E-01	1.01E-01	3.51E-02	1.28E-02	8.31E-03	0.0	4.06E-03
2.1150 to 2.0700	5.57E-01	3.32E-01	2.33E-01	9.22E-02	6.80E-02	3.74E-02	8.18E-03	0.0
2.0700 to 2.0250	4.24E-01	2.64E-01	2.51E-01	1.23E-01	7.65E-02	2.91E-02	8.18E-03	8.12E-03
2.0250 to 1.9800	2.66E-01	1.63E-01	1.33E-01	1.36E-01	8.50E-02	4.98E-02	2.45E-02	8.12E-03
1.9800 to 1.9350	1.53E-01	1.63E-01	1.37E-01	1.01E-01	5.10E-02	2.91E-02	2.86E-02	4.06E-03
1.9350 to 1.8900	1.23E-01	7.21E-02	5.03E-02	6.58E-02	6.38E-02	2.08E-02	1.64E-02	1.62E-02
1.8900 to 1.8450	5.11E-02	5.77E-02	5.48E-02	2.63E-02	2.13E-02	2.91E-02	8.18E-03	4.06E-03
1.8450 to 1.8000	3.07E-02	6.73E-02	3.66E-02	3.07E-02	2.13E-02	4.15E-02	8.18E-03	4.06E-03
1.8000 to 1.7550	4.60E-02	3.85E-02	3.66E-02	2.63E-02	2.13E-02	4.15E-03	8.18E-03	0.0
1.7550 to 1.7100	1.53E-02	2.88E-02	4.57E-02	1.76E-02	1.70E-02	1.25E-02	4.09E-03	4.06E-03
1.7100 to 1.6650	3.07E-02	1.44E-02	3.66E-02	1.76E-02	1.70E-02	1.66E-02	8.18E-03	0.0
1.6650 to 1.6200	1.53E-02	4.33E-02	1.83E-02	8.78E-03	1.28E-02	0.0	8.18E-03	0.0
1.6200 to 1.5750	0.0	2.40E-02	9.14E-03	0.0	4.25E-03	4.15E-03	4.09E-03	8.12E-03
1.5750 to 1.5300	1.53E-02	1.44E-02	0.0	8.78E-03	1.28E-02	4.15E-03	0.0	4.06E-03
1.5300 to 1.4850	1.02E-02	2.40E-02	4.57E-03	8.78E-03	4.25E-03	0.0	8.18E-03	4.06E-03
1.4850 to 1.4400	0.0	9.61E-03	9.14E-03	8.78E-03	0.0	4.15E-03	4.09E-03	4.06E-03
1.4400 to 1.3950	1.53E-02	0.0	0.0	8.78E-03	0.0	4.15E-03	1.23E-02	0.0
1.3950 to 1.3500	5.11E-03	1.92E-02	0.0	0.0	0.0	0.0	0.0	0.0
1.3500 to 1.3050	5.11E-03	1.44E-02	4.57E-03	0.0	1.28E-02	8.31E-03	0.0	0.0
1.3050 to 1.2600	0.0	9.61E-03	9.14E-03	4.39E-03	0.0	0.0	4.09E-03	0.0
1.2600 to 1.2150	0.0	4.81E-03	4.57E-03	1.32E-02	0.0	0.0	4.09E-03	0.0
1.2150 to 1.1700	3.07E-02	4.81E-03	0.0	0.0	0.0	0.0	4.09E-03	0.0
1.1700 to 1.1250	0.0	0.0	0.0	0.0	4.25E-03	0.0	0.0	4.06E-03
1.1250 to 1.0800	1.02E-02	0.0	4.57E-03	4.39E-03	8.50E-03	0.0	0.0	0.0
1.0800 to 1.0350	5.11E-03	4.81E-03	4.57E-03	0.0	8.50E-03	0.0	4.09E-03	0.0
1.0350 to 0.9900	0.0	0.0	0.0	8.78E-03	0.0	0.0	0.0	0.0
0.9900 to 0.9450	0.0	4.81E-03	4.57E-03	4.39E-03	0.0	0.0	0.0	4.06E-03
0.9450 to 0.9000	0.0	4.81E-03	0.0	4.39E-03	0.0	0.0	0.0	0.0
0.9000 to 0.8550	5.11E-03	0.0	9.14E-03	8.78E-03	0.0	4.15E-03	0.0	0.0
0.8550 to 0.8100	5.11E-03	4.81E-03	0.0	0.0	0.0	0.0	0.0	0.0
0.8100 to 0.7650	5.11E-03	0.0	0.0	4.39E-03	0.0	0.0	0.0	4.06E-03
0.7650 to 0.7200	5.11E-03	0.0	0.0	0.0	4.25E-03	0.0	0.0	0.0
0.7200 to 0.6750	1.53E-02	4.81E-03	4.57E-03	4.39E-03	0.0	0.0	0.0	0.0
0.6750 to 0.6300	1.02E-02	0.0	9.14E-03	0.0	0.0	0.0	0.0	0.0
0.6300 to 0.5850	1.02E-02	0.0	0.0	0.0	0.0	0.0	0.0	4.06E-03
0.5850 to 0.5400	5.11E-03	9.61E-03	9.14E-03	4.39E-03	4.25E-03	4.15E-03	0.0	0.0
0.5400 to 0.4950	0.0	9.61E-03	4.57E-03	0.0	0.0	0.0	0.0	0.0
0.4950 to 0.4500	0.0	4.81E-03	0.0	4.39E-03	4.25E-03	4.15E-03	0.0	0.0
0.4500 to 0.4050	2.04E-02	9.61E-03	0.0	4.39E-03	4.25E-03	4.15E-03	0.0	0.0
0.4050 to 0.3600	1.02E-02	1.44E-02	0.0	4.39E-03	0.0	0.0	0.0	4.06E-03
0.3600 to 0.3150	0.0	9.61E-03	4.57E-03	0.0	0.0	0.0	0.0	0.0
0.3150 to 0.2700	5.11E-03	4.81E-03	9.14E-03	4.39E-03	0.0	0.0	0.0	0.0
0.2700 to 0.2250	5.11E-03	9.61E-03	4.57E-03	4.39E-03	8.50E-03	4.15E-03	0.0	0.0

TABLE III.- ENERGY SPECTRA AND ANGULAR DISTRIBUTION OF ELECTRONS TRANSMITTED THROUGH SILICON SLABS OF VARIOUS THICKNESSES – Continued

(c) Target thickness = 0.23517 CSDA range = 0.3390 g/cm^2

Energy, E, Mev	Angular distributions for θ, deg, of –									
	0.0 to 5.000	5.000 to 10.000	10.000 to 15.000	15.000 to 20.000	20.000 to 25.000	25.000 to 30.000	30.000 to 35.000	35.000 to 40.000	40.000 to 45.000	45.000 to 50.000
2.4300 to 2.3850	0.0	0.0	0.0	0.0	0.0	0.0	0.0	0.0	0.0	0.0
2.3850 to 2.3400	0.0	0.0	0.0	0.0	0.0	0.0	0.0	0.0	0.0	0.0
2.3400 to 2.2950	0.0	0.0	0.0	0.0	0.0	0.0	0.0	0.0	0.0	0.0
2.2950 to 2.2500	0.0	0.0	0.0	0.0	0.0	0.0	0.0	0.0	0.0	0.0
2.2500 to 2.2050	0.0	0.0	0.0	0.0	0.0	0.0	0.0	0.0	0.0	0.0
2.2050 to 2.1600	0.0	0.0	0.0	0.0	0.0	0.0	0.0	0.0	0.0	0.0
2.1600 to 2.1150	0.0	0.0	0.0	0.0	0.0	0.0	0.0	0.0	0.0	0.0
2.1150 to 2.0700	9.29E-02	3.11E-02	1.87E-02	0.0	1.06E-02	0.0	0.0	0.0	0.0	0.0
2.0700 to 2.0250	7.44E-01	4.97E-01	7.12E-01	4.99E-01	3.81E-01	2.81E-01	1.43E-01	8.66E-02	2.40E-02	1.65E-02
2.0250 to 1.9800	2.97E 00	2.98E 00	2.17E 00	2.29E 00	1.51E 00	1.16E 00	1.01E 00	6.19E-01	3.72E-01	2.31E-01
1.9800 to 1.9350	2.97E 00	2.73E 00	2.73E 00	2.51E 00	2.07E 00	1.67E 00	1.32E 00	1.21E 00	9.30E-01	5.72E-01
1.9350 to 1.8900	2.04E 00	2.21E 00	1.54E 00	1.79E 00	1.30E 00	1.41E 00	1.06E 00	1.09E 00	7.08E-01	5.50E-01
1.8900 to 1.8450	6.51E-01	1.18E 00	1.07E 00	9.17E-01	9.32E-01	9.48E-01	7.55E-01	6.99E-01	5.76E-01	5.11E-01
1.8450 to 1.8000	8.36E-01	8.39E-01	5.43E-01	8.49E-01	7.10E-01	7.20E-01	5.89E-01	4.79E-01	3.96E-01	4.12E-01
1.8000 to 1.7550	1.12E 00	6.21E-01	4.50E-01	5.93E-01	4.24E-01	3.51E-01	3.55E-01	4.06E-01	2.76E-01	1.70E-01
1.7550 to 1.7100	3.72E-01	2.80E-01	4.31E-01	4.18E-01	4.77E-01	3.25E-01	2.64E-01	2.80E-01	1.50E-01	1.65E-01
1.7100 to 1.6650	3.72E-01	2.48E-01	4.12E-01	2.56E-01	2.54E-01	2.28E-01	1.51E-01	2.60E-01	1.80E-01	1.65E-01
1.6650 to 1.6200	4.65E-01	2.17E-01	3.18E-01	2.02E-01	2.33E-01	1.84E-01	1.43E-01	1.13E-01	1.50E-01	1.43E-01
1.6200 to 1.5750	2.79E-01	1.24E-01	1.50E-01	1.48E-01	1.80E-01	1.32E-01	8.30E-02	1.60E-01	1.38E-01	1.10E-01
1.5750 to 1.5300	0.0	6.21E-02	1.87E-01	2.29E-01	1.48E-01	1.40E-01	1.21E-01	9.99E-02	9.00E-02	8.25E-02
1.5300 to 1.4850	9.29E-02	1.55E-01	1.50E-01	6.74E-02	9.53E-02	6.15E-02	3.77E-02	9.32E-02	7.80E-02	4.40E-02
1.4850 to 1.4400	9.29E-02	3.11E-02	7.49E-02	9.44E-02	1.06E-01	5.27E-02	8.30E-02	9.32E-02	4.80E-02	7.70E-02
1.4400 to 1.3950	1.86E-01	3.11E-02	1.87E-02	5.39E-02	5.30E-02	2.63E-02	6.04E-02	4.66E-02	6.60E-02	3.30E-02
1.3950 to 1.3500	0.0	0.0	3.75E-02	5.39E-02	1.06E-01	6.15E-02	3.77E-02	3.33E-02	3.60E-02	3.85E-02
1.3500 to 1.3050	9.29E-02	3.11E-02	3.75E-02	1.35E-02	3.18E-02	5.27E-02	4.53E-02	3.33E-02	1.80E-02	6.60E-02
1.3050 to 1.2600	9.29E-02	0.0	1.87E-02	5.39E-02	1.06E-02	4.39E-02	3.77E-02	2.66E-02	3.60E-02	1.10E-02
1.2600 to 1.2150	0.0	1.24E-01	1.87E-02	1.35E-02	2.12E-02	4.39E-02	4.53E-02	3.33E-02	2.40E-02	1.65E-02
1.2150 to 1.1700	0.0	3.11E-02	1.87E-02	0.0	1.06E-02	1.76E-02	1.51E-02	6.66E-02	1.20E-02	2.75E-02
1.1700 to 1.1250	9.29E-02	9.32E-02	1.87E-02	0.0	1.06E-02	5.27E-02	1.51E-02	2.66E-02	1.20E-02	1.10E-02
1.1250 to 1.0800	0.0	3.11E-02	1.87E-02	1.35E-02	2.12E-02	3.51E-02	3.02E-02	1.33E-02	3.00E-02	1.65E-02
1.0800 to 1.0350	0.0	0.0	3.75E-02	4.04E-02	4.24E-02	8.78E-02	7.55E-02	6.66E-02	6.00E-03	2.20E-02
1.0350 to 0.9900	9.29E-02	3.11E-02	1.87E-02	1.35E-02	3.18E-02	0.0	7.55E-02	3.33E-02	1.20E-02	1.10E-02
0.9900 to 0.9450	0.0	3.11E-02	3.75E-02	2.70E-02	0.0	3.51E-02	1.51E-02	3.33E-02	6.00E-03	2.20E-02
0.9450 to 0.9000	0.0	3.11E-02	0.0	0.0	2.12E-02	2.63E-02	3.02E-02	2.00E-02	1.80E-02	2.75E-02
0.9000 to 0.8550	9.29E-02	3.11E-02	3.75E-02	0.0	1.06E-02	8.78E-02	7.55E-02	1.33E-02	2.40E-02	1.10E-02
0.8550 to 0.8100	0.0	0.0	1.87E-02	1.35E-02	3.18E-02	5.27E-02	2.26E-02	1.33E-02	1.80E-02	2.75E-02
0.8100 to 0.7650	0.0	0.0	5.62E-02	2.70E-02	0.0	1.76E-02	1.51E-02	2.66E-02	1.20E-02	2.20E-02
0.7650 to 0.7200	0.0	0.0	1.87E-02	2.70E-02	1.06E-02	0.0	0.0	6.66E-03	1.80E-02	1.65E-02
0.7200 to 0.6750	0.0	3.11E-02	1.87E-02	0.0	3.18E-02	1.76E-02	3.77E-02	1.33E-02	6.00E-03	1.10E-02
0.6750 to 0.6300	0.0	6.21E-02	0.0	2.70E-02	2.12E-02	1.76E-02	1.51E-02	2.00E-02	1.20E-02	0.0
0.6300 to 0.5850	1.86E-01	0.0	1.87E-02	2.70E-02	1.06E-02	1.76E-02	0.0	2.00E-02	2.40E-02	1.10E-02
0.5850 to 0.5400	0.0	0.0	0.0	4.04E-02	1.06E-02	0.0	1.51E-02	6.66E-03	1.20E-02	1.10E-02
0.5400 to 0.4950	9.29E-02	0.0	1.87E-02	1.35E-02	4.24E-02	8.78E-03	1.51E-02	6.66E-03	6.00E-03	1.65E-02
0.4950 to 0.4500	0.0	3.11E-02	0.0	1.35E-02	1.06E-02	1.76E-02	1.51E-02	1.33E-02	6.00E-03	1.10E-02
0.4500 to 0.4050	9.29E-02	0.0	0.0	6.74E-02	2.12E-02	2.63E-02	1.51E-02	2.66E-02	1.20E-02	1.65E-02
0.4050 to 0.3600	0.0	3.11E-02	1.87E-02	1.35E-02	0.0	3.51E-02	1.51E-02	2.66E-02	1.80E-02	0.0
0.3600 to 0.3150	0.0	0.0	0.0	0.0	4.24E-02	2.63E-02	0.0	2.66E-02	1.20E-02	0.0
0.3150 to 0.2700	0.0	6.21E-02	1.87E-02	0.0	2.12E-02	0.0	7.55E-03	6.66E-03	1.20E-02	1.10E-02
0.2700 to 0.2250	0.0	0.0	5.62E-02	0.0	1.06E-02	8.78E-03	1.51E-02	1.33E-02	2.40E-02	1.10E-02

TABLE III.- ENERGY SPECTRA AND ANGULAR DISTRIBUTION OF ELECTRONS TRANSMITTED THROUGH SILICON SLABS OF VARIOUS THICKNESSES – Continued

(c) Target thickness = 0.23517 CSDA range = 0.3390 g/cm^2 – Concluded

Energy, E, Mev	Angular distributions for θ, deg, of –							
	50.000 to 55.000	55.000 to 60.000	60.000 to 65.000	65.000 to 70.000	70.000 to 75.000	75.000 to 80.000	80.000 to 85.000	85.000 to 90.000
2.4300 to 2.3850	0.0	0.0	0.0	0.0	0.0	0.0	0.0	0.0
2.3850 to 2.3400	0.0	0.0	0.0	0.0	0.0	0.0	0.0	0.0
2.3400 to 2.2950	0.0	0.0	0.0	0.0	0.0	0.0	0.0	0.0
2.2950 to 2.2500	0.0	0.0	0.0	0.0	0.0	0.0	0.0	0.0
2.2500 to 2.2050	0.0	0.0	0.0	0.0	0.0	0.0	0.0	0.0
2.2050 to 2.1600	0.0	0.0	0.0	0.0	0.0	0.0	0.0	0.0
2.1600 to 2.1150	0.0	0.0	0.0	0.0	0.0	0.0	0.0	0.0
2.1150 to 2.0700	0.0	0.0	0.0	0.0	0.0	0.0	0.0	0.0
2.0700 to 2.0250	5.11E-03	4.81E-03	9.14E-03	0.0	0.0	0.0	0.0	0.0
2.0250 to 1.9800	1.69E-01	8.65E-02	5.94E-02	3.07E-02	0.0	4.15E-03	4.09E-03	0.0
1.9800 to 1.9350	3.53E-01	2.36E-01	1.37E-01	5.27E-02	1.70E-02	1.25E-02	4.09E-03	4.06E-03
1.9350 to 1.8900	4.34E-01	2.93E-01	2.24E-01	6.58E-02	8.08E-02	2.49E-02	1.64E-02	4.06E-03
1.8900 to 1.8450	3.88E-01	2.55E-01	2.01E-01	1.80E-01	1.19E-01	4.15E-02	1.23E-02	4.06E-03
1.8450 to 1.8000	3.12E-01	2.07E-01	2.33E-01	1.71E-01	8.50E-02	4.98E-02	6.95E-02	1.62E-02
1.8000 to 1.7550	2.30E-01	2.21E-01	1.74E-01	1.18E-01	9.78E-02	6.64E-02	3.68E-02	2.03E-02
1.7550 to 1.7100	1.94E-01	1.44E-01	1.14E-01	1.18E-01	7.23E-02	4.57E-02	5.32E-02	1.62E-02
1.7100 to 1.6650	1.38E-01	1.30E-01	1.05E-01	1.10E-01	5.10E-02	3.74E-02	2.86E-02	4.06E-03
1.6650 to 1.6200	1.23E-01	7.21E-02	1.10E-01	6.14E-02	5.95E-02	1.66E-02	3.27E-02	8.12E-03
1.6200 to 1.5750	1.12E-01	5.77E-02	6.40E-02	7.02E-02	4.68E-02	3.74E-02	8.18E-03	1.22E-02
1.5750 to 1.5300	6.64E-02	6.25E-02	6.40E-02	6.14E-02	2.13E-02	2.91E-02	1.23E-02	8.12E-03
1.5300 to 1.4850	4.09E-02	3.36E-02	5.03E-02	3.95E-02	4.68E-02	1.25E-02	1.23E-02	1.22E-02
1.4850 to 1.4400	3.07E-02	4.81E-02	2.74E-02	4.83E-02	3.83E-02	1.66E-02	1.64E-02	4.06E-03
1.4400 to 1.3950	2.04E-02	2.40E-02	3.66E-02	3.51E-02	2.13E-02	1.66E-02	1.64E-02	4.06E-03
1.3950 to 1.3500	4.09E-02	2.40E-02	1.83E-02	3.07E-02	1.70E-02	1.66E-02	4.09E-03	0.0
1.3500 to 1.3050	2.04E-02	2.40E-02	1.37E-02	1.76E-02	1.70E-02	1.66E-02	8.18E-03	8.12E-03
1.3050 to 1.2600	3.07E-02	3.36E-02	9.14E-03	2.19E-02	1.70E-02	2.08E-02	0.0	4.06E-03
1.2600 to 1.2150	3.07E-02	4.33E-02	9.14E-03	8.78E-03	8.50E-03	1.25E-02	4.09E-03	0.0
1.2150 to 1.1700	1.53E-02	4.81E-03	2.74E-02	1.76E-02	8.50E-03	1.25E-02	0.0	4.06E-03
1.1700 to 1.1250	0.0	2.88E-02	2.74E-02	1.32E-02	4.25E-03	0.0	4.09E-03	4.06E-03
1.1250 to 1.0800	2.04E-02	1.44E-02	0.0	1.32E-02	8.50E-03	4.15E-03	8.18E-03	0.0
1.0800 to 1.0350	3.07E-02	4.81E-03	1.37E-02	1.76E-02	8.50E-03	4.15E-03	0.0	0.0
1.0350 to 0.9900	2.04E-02	2.40E-02	9.14E-03	8.78E-03	4.25E-03	0.0	0.0	8.12E-03
0.9900 to 0.9450	4.60E-02	9.61E-03	1.37E-02	1.32E-02	1.28E-02	4.15E-03	4.09E-03	0.0
0.9450 to 0.9000	1.53E-02	1.44E-02	9.14E-03	8.78E-03	4.25E-03	0.0	0.0	0.0
0.9000 to 0.8550	1.02E-02	0.0	1.37E-02	8.78E-03	8.50E-03	1.25E-02	0.0	0.0
0.8550 to 0.8100	1.02E-02	9.61E-03	1.37E-02	0.0	1.28E-02	0.0	0.0	0.0
0.8100 to 0.7650	2.04E-02	4.81E-03	9.14E-03	0.0	0.0	8.31E-03	4.09E-03	0.0
0.7650 to 0.7200	0.0	0.0	0.0	4.39E-03	4.25E-03	4.15E-03	0.0	4.06E-03
0.7200 to 0.6750	1.53E-02	9.61E-03	0.0	1.76E-02	4.25E-03	0.0	0.0	0.0
0.6750 to 0.6300	1.02E-02	0.0	4.57E-03	4.39E-03	0.0	0.0	0.0	4.06E-03
0.6300 to 0.5850	1.02E-02	0.0	9.14E-03	4.39E-03	0.0	4.15E-03	0.0	4.06E-03
0.5850 to 0.5400	5.11E-03	4.81E-03	4.57E-03	8.78E-03	4.25E-03	0.0	4.09E-03	0.0
0.5400 to 0.4950	5.11E-03	1.44E-02	9.14E-03	4.39E-03	0.0	0.0	4.09E-03	0.0
0.4950 to 0.4500	5.11E-03	9.61E-03	4.57E-03	0.0	4.25E-03	0.0	0.0	0.0
0.4500 to 0.4050	5.11E-03	4.81E-03	1.37E-02	0.0	4.25E-03	4.15E-03	4.09E-03	0.0
0.4050 to 0.3600	0.0	1.92E-02	1.37E-02	1.32E-02	4.25E-03	0.0	4.09E-03	4.06E-03
0.3600 to 0.3150	1.02E-02	4.81E-03	1.83E-02	0.0	0.0	4.15E-03	0.0	0.0
0.3150 to 0.2700	1.02E-02	4.81E-03	9.14E-03	1.32E-02	0.0	4.15E-03	0.0	0.0
0.2700 to 0.2250	1.02E-02	1.44E-02	9.14E-03	4.39E-03	4.25E-03	4.15E-03	4.09E-03	0.0

TABLE III.- ENERGY SPECTRA AND ANGULAR DISTRIBUTION OF ELECTRONS TRANSMITTED THROUGH SILICON SLABS OF VARIOUS THICKNESSES – Continued

(d) Target thickness = 0.39195 CSDA range = 0.5650 g/cm^2

Energy, E, Mev	Angular distributions for θ, deg, of –									
	0.0 to 5.000	5.000 to 10.000	10.000 to 15.000	15.000 to 20.000	20.000 to 25.000	25.000 to 30.000	30.000 to 35.000	35.000 to 40.000	40.000 to 45.000	45.000 to 50.000
2.4300 to 2.3850	0.0	0.0	0.0	0.0	0.0	0.0	0.0	0.0	0.0	0.0
2.3850 to 2.3400	0.0	0.0	0.0	0.0	0.0	0.0	0.0	0.0	0.0	0.0
2.3400 to 2.2950	0.0	0.0	0.0	0.0	0.0	0.0	0.0	0.0	0.0	0.0
2.2950 to 2.2500	0.0	0.0	0.0	0.0	0.0	0.0	0.0	0.0	0.0	0.0
2.2500 to 2.2050	0.0	0.0	0.0	0.0	0.0	0.0	0.0	0.0	0.0	0.0
2.2050 to 2.1600	0.0	0.0	0.0	0.0	0.0	0.0	0.0	0.0	0.0	0.0
2.1600 to 2.1150	0.0	0.0	0.0	0.0	0.0	0.0	0.0	0.0	0.0	0.0
2.1150 to 2.0700	0.0	0.0	0.0	0.0	0.0	0.0	0.0	0.0	0.0	0.0
2.0700 to 2.0250	0.0	0.0	0.0	0.0	0.0	0.0	0.0	0.0	0.0	0.0
2.0250 to 1.9800	0.0	0.0	0.0	0.0	0.0	0.0	0.0	0.0	0.0	0.0
1.9800 to 1.9350	0.0	0.0	0.0	0.0	0.0	0.0	0.0	0.0	0.0	0.0
1.9350 to 1.8900	0.0	0.0	0.0	0.0	0.0	0.0	0.0	0.0	0.0	0.0
1.8900 to 1.8350	0.0	0.0	0.0	0.0	0.0	0.0	0.0	0.0	0.0	0.0
1.8450 to 1.8000	0.0	0.0	0.0	0.0	0.0	0.0	0.0	0.0	0.0	0.0
1.8000 to 1.7550	9.29E-02	0.0	1.87E-02	4.04E-02	5.30E-02	8.78E-03	7.55E-03	2.00E-02	0.0	0.0
1.7550 to 1.7100	2.79E-01	3.42E-01	2.25E-01	1.62E-01	1.27E-01	1.23E-01	6.79E-02	8.66E-02	7.20E-02	2.20E-02
1.7100 to 1.6650	2.79E-01	7.76E-01	4.12E-01	4.18E-01	3.39E-01	3.86E-01	2.79E-01	1.86E-01	1.38E-01	1.21E-01
1.6650 to 1.6200	8.36E-01	6.52E-01	7.49E-01	6.34E-01	4.87E-01	4.48E-01	4.07E-01	2.40E-01	2.52E-01	1.81E-01
1.6200 to 1.5750	9.29E-01	7.77E-01	7.87E-01	8.63E-01	6.04E-01	5.97E-01	4.68E-01	2.86E-01	3.18E-01	2.14E-01
1.5750 to 1.5300	3.72E-01	1.06E 00	7.12E-01	6.34E-01	6.04E-01	5.88E-01	6.26E-01	3.80E-01	3.60E-01	2.36E-01
1.5300 to 1.4850	6.51E-01	5.59E-01	6.37E-01	7.01E-01	5.19E-01	4.83E-01	4.68E-01	3.73E-01	3.18E-01	1.70E-01
1.4850 to 1.4400	4.65E-01	6.52E-01	5.24E-01	4.85E-01	5.19E-01	3.95E-01	4.23E-01	3.93E-01	2.40E-01	2.69E-01
1.4400 to 1.3950	5.58E-01	4.35E-01	3.37E-01	2.70E-01	3.60E-01	3.69E-01	4.23E-01	3.20E-01	2.40E-01	2.09E-01
1.3950 to 1.3500	4.65E-01	2.48E-01	3.37E-01	2.97E-01	3.60E-01	2.99E-01	2.49E-01	2.86E-01	1.86E-01	1.59E-01
1.3500 to 1.3050	5.58E-01	3.11E-01	2.81E-01	2.29E-01	3.28E-01	3.34E-01	2.34E-01	1.93E-01	2.10E-01	1.70E-01
1.3050 to 1.2600	9.29E-02	9.32E-02	2.44E-01	2.29E-01	2.22E-01	1.58E-01	2.04E-01	1.86E-01	1.86E-01	1.43E-01
1.2600 to 1.2150	9.29E-02	2.80E-01	1.31E-01	1.89E-01	2.01E-01	2.37E-01	1.58E-01	2.46E-01	2.04E-01	1.48E-01
1.2150 to 1.1700	3.72E-01	1.55E-01	2.06E-01	1.21E-01	2.12E-01	1.84E-01	1.21E-01	1.47E-01	1.08E-01	1.43E-01
1.1700 to 1.1250	9.29E-02	9.32E-02	1.12E-01	1.62E-01	1.91E-01	1.49E-01	7.55E-02	1.20E-01	9.00E-02	1.15E-01
1.1250 to 1.0800	1.86E-01	2.80E-01	5.62E-02	8.09E-02	6.36E-02	7.90E-02	1.21E-01	8.66E-02	8.40E-02	1.21E-01
1.0800 to 1.0350	9.29E-02	2.17E-01	7.49E-02	1.21E-01	1.17E-01	1.05E-01	9.05E-02	9.99E-02	9.00E-02	6.60E-02
1.0350 to 0.9900	0.0	1.55E-01	1.69E-01	1.35E-02	9.53E-02	9.66E-02	7.55E-02	4.66E-02	1.38E-01	3.85E-02
0.9900 to 0.9450	9.29E-02	9.32E-02	5.62E-02	1.08E-01	5.30E-02	7.02E-02	3.02E-02	5.33E-02	7.20E-02	7.15E-02
0.9450 to 0.9000	9.29E-02	0.0	1.87E-02	8.09E-02	6.36E-02	1.76E-02	8.30E-02	6.66E-02	6.60E-02	2.75E-02
0.9000 to 0.8550	9.29E-02	3.11E-02	1.87E-02	9.44E-02	6.36E-02	5.27E-02	7.55E-02	5.33E-02	6.60E-02	7.15E-02
0.8550 to 0.8100	1.86E-01	1.24E-01	7.49E-02	9.44E-02	4.24E-02	8.78E-02	9.81E-02	6.66E-02	1.80E-02	3.85E-02
0.8100 to 0.7650	0.0	0.0	1.87E-02	4.04E-02	4.24E-02	2.63E-02	6.79E-02	3.33E-02	1.80E-02	3.30E-02
0.7650 to 0.7200	0.0	9.32E-02	5.62E-02	1.35E-01	4.24E-02	4.39E-02	2.26E-02	5.33E-02	2.40E-02	5.50E-02
0.7200 to 0.6750	1.86E-01	0.0	1.87E-02	5.39E-02	7.42E-02	3.51E-02	8.30E-02	6.66E-02	3.60E-02	2.20E-02
0.6750 to 0.6300	0.0	0.0	5.62E-02	1.35E-02	4.24E-02	5.27E-02	6.79E-02	3.33E-02	3.00E-02	4.95E-02
0.6300 to 0.5850	0.0	0.0	3.75E-02	6.74E-02	4.24E-02	6.15E-02	3.02E-02	2.66E-02	1.20E-02	1.65E-02
0.5850 to 0.5400	0.0	6.21E-02	5.62E-02	2.70E-02	6.36E-02	4.39E-02	3.77E-02	2.00E-02	1.20E-02	3.30E-02
0.5400 to 0.4950	9.29E-02	0.0	1.87E-02	1.35E-02	3.18E-02	3.51E-02	3.02E-02	2.66E-02	3.00E-02	1.10E-02
0.4950 to 0.4500	0.0	3.11E-02	5.62E-02	6.74E-02	4.24E-02	3.51E-02	3.77E-02	4.00E-02	3.00E-02	1.65E-02
0.4500 to 0.4050	0.0	6.21E-02	0.0	1.35E-02	4.24E-02	1.76E-02	7.55E-03	3.33E-02	1.80E-02	1.10E-02
0.4050 to 0.3600	0.0	9.32E-02	1.87E-02	1.35E-02	2.12E-02	4.39E-02	7.55E-03	4.66E-02	4.20E-02	2.75E-02
0.3600 to 0.3150	9.29E-02	3.11E-02	7.49E-02	9.44E-02	3.18E-02	5.27E-02	3.77E-02	2.00E-02	6.00E-03	1.65E-02
0.3150 to 0.2700	0.0	3.11E-02	5.62E-02	2.70E-02	2.12E-02	3.51E-02	6.04E-02	2.66E-02	0.0	1.65E-02
0.2700 to 0.2250	0.0	6.21E-02	3.75E-02	2.70E-02	1.06E-02	6.15E-02	1.51E-02	1.33E-02	4.80E-02	1.10E-02

TABLE III.- ENERGY SPECTRA AND ANGULAR DISTRIBUTION OF ELECTRONS TRANSMITTED THROUGH SILICON SLABS OF VARIOUS THICKNESSES – Continued

(d) Target thickness = 0.39195 CSDA range = 0.5650 g/cm^2 – Concluded

Energy, E, MeV	Angular distributions for θ, deg, of –							
	50.000 to 55.000	55.000 to 60.000	60.000 to 65.000	65.000 to 70.000	70.000 to 75.000	75.000 to 80.000	80.000 to 85.000	85.000 to 90.000
2.4300 to 2.3850	0.0	0.0	0.0	0.0	0.0	0.0	0.0	0.0
2.3850 to 2.3400	0.0	0.0	0.0	0.0	0.0	0.0	0.0	0.0
2.3400 to 2.2950	0.0	0.0	0.0	0.0	0.0	0.0	0.0	0.0
2.2950 to 2.2500	0.0	0.0	0.0	0.0	0.0	0.0	0.0	0.0
2.2500 to 2.2050	0.0	0.0	0.0	0.0	0.0	0.0	0.0	0.0
2.2050 to 2.1600	0.0	0.0	0.0	0.0	0.0	0.0	0.0	0.0
2.1600 to 2.1150	0.0	0.0	0.0	0.0	0.0	0.0	0.0	0.0
2.1150 to 2.0700	0.0	0.0	0.0	0.0	0.0	0.0	0.0	0.0
2.0700 to 2.0250	0.0	0.0	0.0	0.0	0.0	0.0	0.0	0.0
2.0250 to 1.9800	0.0	0.0	0.0	0.0	0.0	0.0	0.0	0.0
1.9800 to 1.9350	0.0	0.0	0.0	0.0	0.0	0.0	0.0	0.0
1.9350 to 1.8900	0.0	0.0	0.0	0.0	0.0	0.0	0.0	0.0
1.8900 to 1.8450	0.0	0.0	0.0	0.0	0.0	0.0	0.0	0.0
1.8450 to 1.8000	0.0	0.0	0.0	0.0	0.0	0.0	0.0	0.0
1.8000 to 1.7500	5.11E-03	4.81E-03	0.0	0.0	0.0	0.0	0.0	0.0
1.7550 to 1.7100	5.11E-03	9.61E-03	9.14E-03	8.78E-03	1.28E-02	0.0	4.09E-03	0.0
1.7100 to 1.6650	9.71E-02	2.40E-02	3.20E-02	8.78E-03	1.70E-02	1.25E-02	4.09E-03	0.0
1.6650 to 1.6200	9.71E-02	5.77E-02	6.86E-02	1.32E-02	8.50E-03	8.31E-03	0.0	4.06E-03
1.6200 to 1.5750	1.74E-01	1.39E-01	6.86E-02	6.58E-02	4.25E-02	1.25E-02	4.09E-03	8.12E-03
1.5750 to 1.5300	1.74E-01	1.63E-01	1.46E-01	9.22E-02	3.83E-02	2.08E-02	8.18E-03	4.06E-03
1.5300 to 1.4850	1.94E-01	1.59E-01	1.42E-01	9.65E-02	4.25E-02	2.91E-02	2.86E-02	0.0
1.4850 to 1.4400	2.40E-01	1.59E-01	1.05E-01	7.46E-02	5.10E-02	2.91E-02	2.86E-02	8.12E-03
1.4400 to 1.3950	2.10E-01	1.11E-01	1.05E-01	8.34E-02	5.10E-02	2.49E-02	1.64E-02	1.62E-02
1.3950 to 1.3500	1.79E-01	1.20E-01	6.86E-02	5.70E-02	6.38E-02	4.98E-02	1.23E-02	4.06E-03
1.3500 to 1.3050	1.94E-01	1.06E-01	1.14E-01	6.14E-02	6.38E-02	2.91E-02	2.04E-02	8.12E-03
1.3050 to 1.2600	1.58E-01	1.39E-01	9.60E-02	8.34E-02	8.93E-02	2.49E-02	2.04E-02	1.22E-02
1.2600 to 1.2150	9.20E-02	1.11E-01	6.86E-02	5.70E-02	2.55E-02	4.15E-02	2.86E-02	4.06E-03
1.2150 to 1.1700	1.28E-01	8.17E-02	5.48E-02	5.70E-02	8.08E-02	4.15E-02	2.45E-02	1.62E-02
1.1700 to 1.1250	1.43E-01	4.81E-02	7.77E-02	4.83E-02	3.40E-02	2.49E-02	2.04E-02	8.12E-03
1.1250 to 1.0800	6.13E-02	5.29E-02	8.23E-02	5.27E-02	4.68E-02	2.91E-02	1.64E-02	8.12E-03
1.0800 to 1.0350	8.69E-02	1.01E-01	6.40E-02	3.07E-02	3.40E-02	2.91E-02	0.0	1.22E-02
1.0350 to 0.9900	4.09E-02	4.33E-02	3.20E-02	4.83E-02	2.55E-02	2.49E-02	1.23E-02	8.12E-03
0.9900 to 0.9450	3.07E-02	7.21E-02	2.29E-02	3.51E-02	2.13E-02	1.66E-02	1.23E-02	4.06E-03
0.9450 to 0.9000	5.62E-02	5.29E-02	2.74E-02	3.07E-02	3.40E-02	2.08E-02	4.09E-03	4.06E-03
0.9000 to 0.8550	7.67E-02	6.73E-02	3.66E-02	3.07E-02	2.13E-02	2.08E-02	1.23E-02	8.12E-03
0.8550 to 0.8100	2.56E-02	9.61E-03	2.29E-02	2.63E-02	2.55E-02	4.15E-03	4.09E-03	4.06E-03
0.8100 to 0.7650	6.64E-02	9.61E-03	1.83E-02	1.32E-02	2.13E-02	1.25E-02	0.0	0.0
0.7650 to 0.7200	2.04E-02	3.36E-02	1.37E-02	1.76E-02	2.13E-02	1.66E-02	1.23E-02	4.06E-03
0.7200 to 0.6750	3.07E-02	2.88E-02	1.37E-02	3.51E-02	1.70E-02	0.0	8.18E-03	0.0
0.6750 to 0.6300	4.09E-02	4.33E-02	4.57E-03	1.76E-02	1.70E-02	0.0	4.09E-03	0.0
0.6300 to 0.5850	1.53E-02	3.85E-02	1.37E-02	3.51E-02	1.28E-02	0.0	0.0	4.06E-03
0.5850 to 0.5400	1.53E-02	9.61E-03	2.29E-02	1.76E-02	1.70E-02	1.25E-02	0.0	8.12E-03
0.5400 to 0.4950	2.56E-02	0.0	2.29E-02	1.32E-02	8.50E-03	0.0	4.09E-03	0.0
0.4950 to 0.4500	1.02E-02	2.88E-02	9.14E-03	1.76E-02	4.25E-03	8.31E-03	4.09E-03	4.06E-03
0.4500 to 0.4050	1.53E-02	9.61E-03	9.14E-03	1.32E-02	1.70E-02	0.0	8.18E-03	4.06E-03
0.4050 to 0.3600	2.56E-02	1.92E-02	1.83E-02	1.32E-02	8.50E-03	4.15E-03	1.23E-02	0.0
0.3600 to 0.3150	1.02E-02	1.92E-02	1.37E-02	3.07E-02	8.50E-03	1.25E-02	0.0	0.0
0.3150 to 0.2700	2.56E-02	1.44E-02	1.83E-02	1.32E-02	1.28E-02	0.0	4.09E-03	0.0
0.2700 to 0.2250	0.0	4.81E-03	0.0	1.32E-02	0.0	4.15E-03	0.0	4.06E-03

TABLE III.- ENERGY SPECTRA AND ANGULAR DISTRIBUTION OF ELECTRONS TRANSMITTED THROUGH SILICON SLABS OF VARIOUS THICKNESSES – Continued

(e) Target thickness = 0.47034 CSDA range = 0.6780 g/cm^2

Energy, E, MeV	Angular distributions for θ, deg, of –									
	0.0 to 5.000	5.000 to 10.000	10.000 to 15.000	15.000 to 20.000	20.000 to 25.000	25.000 to 30.000	30.000 to 35.000	35.000 to 40.000	40.000 to 45.000	45.000 to 50.000
2.4300 to 2.3850	0.0	0.0	0.0	0.0	0.0	0.0	0.0	0.0	0.0	0.0
2.3850 to 2.3400	0.0	0.0	0.0	0.0	0.0	0.0	0.0	0.0	0.0	0.0
2.3400 to 2.2950	0.0	0.0	0.0	0.0	0.0	0.0	0.0	0.0	0.0	0.0
2.2950 to 2.2500	0.0	0.0	0.0	0.0	0.0	0.0	0.0	0.0	0.0	0.0
2.2500 to 2.2050	0.0	0.0	0.0	0.0	0.0	0.0	0.0	0.0	0.0	0.0
2.2050 to 2.1600	0.0	0.0	0.0	0.0	0.0	0.0	0.0	0.0	0.0	0.0
2.1600 to 2.1150	0.0	0.0	0.0	0.0	0.0	0.0	0.0	0.0	0.0	0.0
2.1150 to 2.0700	0.0	0.0	0.0	0.0	0.0	0.0	0.0	0.0	0.0	0.0
2.0700 to 2.0250	0.0	0.0	0.0	0.0	0.0	0.0	0.0	0.0	0.0	0.0
2.0250 to 1.9800	0.0	0.0	0.0	0.0	0.0	0.0	0.0	0.0	0.0	0.0
1.9800 to 1.9350	0.0	0.0	0.0	0.0	0.0	0.0	0.0	0.0	0.0	0.0
1.9350 to 1.8900	0.0	0.0	0.0	0.0	0.0	0.0	0.0	0.0	0.0	0.0
1.8900 to 1.8450	0.0	0.0	0.0	0.0	0.0	0.0	0.0	0.0	0.0	0.0
1.8450 to 1.8000	0.0	0.0	0.0	0.0	0.0	0.0	0.0	0.0	0.0	0.0
1.8000 to 1.7550	0.0	0.0	0.0	0.0	0.0	0.0	0.0	0.0	0.0	0.0
1.7550 to 1.7100	0.0	0.0	0.0	0.0	0.0	0.0	0.0	0.0	0.0	0.0
1.7100 to 1.6650	0.0	0.0	0.0	0.0	0.0	0.0	0.0	0.0	0.0	0.0
1.6650 to 1.6200	0.0	0.0	0.0	2.70E-02	1.06E-02	8.78E-03	0.0	0.0	0.0	0.0
1.6200 to 1.5750	9.29E-02	6.21E-02	1.12E-01	6.74E-02	4.24E-02	4.39E-02	5.28E-02	6.66E-03	0.0	0.0
1.5750 to 1.5300	0.0	2.80E-01	1.50E-01	1.35E-01	8.48E-02	1.14E-01	6.04E-02	7.33E-02	3.00E-02	3.85E-02
1.5300 to 1.4850	8.36E-01	5.28E-01	3.00E-01	2.02E-01	2.86E-01	1.49E-01	2.34E-01	1.40E-01	1.20E-01	5.50E-02
1.4850 to 1.4400	2.79E-01	4.04E-01	5.24E-01	4.04E-01	3.07E-01	2.90E-01	2.41E-01	2.20E-01	9.00E-02	1.04E-01
1.4400 to 1.3950	6.51E-01	3.42E-01	5.24E-01	3.91E-01	3.50E-01	2.63E-01	2.41E-01	2.40E-01	1.74E-01	1.21E-01
1.3950 to 1.3500	3.72E-01	5.28E-01	5.24E-01	2.83E-01	4.13E-01	2.81E-01	2.11E-01	3.00E-01	1.98E-01	1.76E-01
1.3500 to 1.3050	4.65E-01	4.97E-01	3.75E-01	3.10E-01	4.87E-01	2.99E-01	2.49E-01	2.53E-01	2.76E-01	2.14E-01
1.3050 to 1.2600	3.72E-01	2.17E-01	3.75E-01	3.10E-01	3.18E-01	2.81E-01	3.24E-01	2.13E-01	1.80E-01	1.98E-01
1.2600 to 1.2150	5.58E-01	4.35E-01	3.56E-01	3.24E-01	2.65E-01	4.13E-01	2.41E-01	2.46E-01	1.68E-01	1.87E-01
1.2150 to 1.1700	1.86E-01	2.17E-01	3.37E-01	2.83E-01	2.54E-01	1.93E-01	1.96E-01	1.73E-01	2.46E-01	1.48E-01
1.1700 to 1.1250	3.72E-01	2.17E-01	3.00E-01	3.37E-01	2.54E-01	2.46E-01	2.57E-01	2.26E-01	1.62E-01	1.43E-01
1.1250 to 1.0800	9.29E-02	3.42E-01	2.25E-01	2.29E-01	1.70E-01	1.32E-01	2.49E-01	1.93E-01	1.38E-01	1.15E-01
1.0800 to 1.0350	9.29E-02	1.86E-01	2.44E-01	1.89E-01	1.17E-01	1.58E-01	1.28E-01	1.53E-01	1.44E-01	1.21E-01
1.0350 to 0.9900	2.79E-01	2.48E091	2.81E-01	1.08E-01	1.38E-01	2.02E-01	1.28E-01	1.93E-01	1.38E-01	1.10E-01
0.9900 to 0.9450	0.0	2.17E-01	1.50E-01	1.89E-01	1.17E-01	1.14E-01	9.81E-01	7.99E-02	3.60E-02	1.04E-01
0.9450 to 0.9000	1.86E-01	6.21E-02	9.37E-02	9.44E-02	1.38E-01	1.32E-01	1.06E-01	1.66E-01	1.38E-01	6.60E-02
0.9000 to 0.8550	0.0	1.86E-01	1.12E-01	6.74E-02	6.36E-02	1.23E-01	5.28E-02	9.99E-02	9.60E-02	2.75E-02
0.8550 to 0.8100	1.86E-01	1.24E-01	9.37E-02	1.08E-01	7.42E-02	1.40E-01	6.79E-02	6.66E-02	6.60E-02	9.35E-02
0.8100 to 0.7650	1.86E-01	6.21E-02	1.12E-01	1.48E-01	8.48E-02	4.39E-02	8.30E-02	4.00E-02	4.20E-02	7.70E-02
0.7650 to 0.7200	9.29E-02	1.24E-01	5.62E-02	8.09E-02	1.17E-01	5.27E-02	6.04E-02	1.13E-01	8.40E-02	2.75E-02
0.7200 to 0.6750	9.29E-02	1.24E-01	9.37E-02	6.75E-02	7.42E-02	8.78E-02	6.79E-02	2.00E-02	1.80E-02	6.05E-02
0.6750 to 0.6300	0.0	6.21E-02	1.31E-01	8.09E-02	2.12E-02	1.49E-01	6.04E-02	4.00E-02	3.00E-02	3.30E-02
0.6300 to 0.5850	2.79E-01	3.11E-02	1.12E-01	1.21E-01	2.12E-02	4.39E-02	5.28E-02	4.66E-02	6.00E-02	3.85E-02
0.5850 to 0.5400	0.0	6.21E-02	9.37E-02	8.09E-02	4.24E-02	4.39E-02	2.26E-02	5.33E-02	7.20E-02	2.75E-02
0.5400 to 0.4950	2.79E-01	3.11E-02	3.75E-02	1.35E-02	6.36E-02	7.90E-02	7.55E-02	4.66E-02	3.60E-02	3.30E-02
0.4950 to 0.4500	1.86E-01	6.21E-02	5.62E-02	6.74E-02	4.24E-02	4.39E-02	6.04E-02	5.33E-02	4.80E-02	2.75E-02
0.4500 to 0.4050	0.0	3.11E-02	3.75E-02	8.09E-02	4.24E-02	6.15E-02	2.26E-02	4.00E-02	4.80E-02	1.10E-02
0.4050 to 0.3600	9.29E-02	0.0	5.62E-02	4.04E-02	4.24E-02	1.76E-02	4.53E-02	2.00E-02	1.80E-02	4.40E-02
0.3600 to 0.3150	1.86E-01	3.11E-02	5.62E-02	5.39E-02	6.36E-02	2.63E-02	7.55E-02	2.00E-02	2.40E-02	2.20E-02
0.3150 to 0.2700	0.0	6.21E-02	3.75E-02	1.35E-02	5.30E-02	2.63E-02	3.02E-02	2.00E-02	2.40E-02	1.65E-02
0.2700 to 0.2250	0.0	9.32E-02	1.87E-02	0.0	5.30E-02	5.27E-02	5.28E-02	2.00E-02	6.00E-03	0.0

TABLE III.- ENERGY SPECTRA AND ANGULAR DISTRIBUTION OF ELECTRONS TRANSMITTED THROUGH SILICON SLABS OF VARIOUS THICKNESSES – Concluded

(e) Target thickness = 0.47034 CSDA range = 0.6780 g/cm^2 – Concluded

Energy, E, Mev	Angular distributions for θ, deg, of –							
	50.000 to 55.000	55.000 to 60.000	60.000 to 65.000	65.000 to 70.000	70.000 to 75.000	75.000 to 80.000	80.000 to 85.000	85.000 to 90.000
2.4300 to 2.3850	0.0	0.0	0.0	0.0	0.0	0.0	0.0	0.0
2.3850 to 2.3400	0.0	0.0	0.0	0.0	0.0	0.0	0.0	0.0
2.3400 to 2.2950	0.0	0.0	0.0	0.0	0.0	0.0	0.0	0.0
2.2950 to 2.2500	0.0	0.0	0.0	0.0	0.0	0.0	0.0	0.0
2.2500 to 2.2050	0.0	0.0	0.0	0.0	0.0	0.0	0.0	0.0
2.2050 to 2.1600	0.0	0.0	0.0	0.0	0.0	0.0	0.0	0.0
2.1600 to 2.1150	0.0	0.0	0.0	0.0	0.0	0.0	0.0	0.0
2.1150 to 2.0700	0.0	0.0	0.0	0.0	0.0	0.0	0.0	0.0
2.0700 to 2.0250	0.0	0.0	0.0	0.0	0.0	0.0	0.0	0.0
2.0250 to 1.9800	0.0	0.0	0.0	0.0	0.0	0.0	0.0	0.0
1.9800 to 1.9350	0.0	0.0	0.0	0.0	0.0	0.0	0.0	0.0
1.9350 to 1.8900	0.0	0.0	0.0	0.0	0.0	0.0	0.0	0.0
1.8900 to 1.8450	0.0	0.0	0.0	0.0	0.0	0.0	0.0	0.0
1.8450 to 1.8000	0.0	0.0	0.0	0.0	0.0	0.0	0.0	0.0
1.8000 to 1.7550	0.0	0.0	0.0	0.0	0.0	0.0	0.0	0.0
1.7550 to 1.7100	0.0	0.0	0.0	0.0	0.0	0.0	0.0	0.0
1.7100 to 1.6650	0.0	0.0	0.0	0.0	0.0	0.0	0.0	0.0
1.6650 to 1.6200	0.0	0.0	0.0	0.0	0.0	0.0	0.0	0.0
1.6200 to 1.5750	0.0	4.81E-03	0.0	0.0	0.0	0.0	0.0	0.0
1.5750 to 1.5300	2.56E-02	9.61E-03	4.57E-03	1.32E-02	0.0	0.0	0.0	0.0
1.5300 to 1.4850	2.56E-02	1.92E-02	2.29E-02	8.78E-03	0.0	0.0	0.0	1.22E-02
1.4850 to 1.4400	1.18E-01	6.73E-02	2.74E-02	2.19E-02	4.25E-03	2.08E-02	4.09E-03	8.12E-03
1.4400 to 1.3950	1.43E-01	7.21E-02	3.20E-02	4.39E-02	1.28E-02	1.66E-02	4.09E-03	0.0
1.3950 to 1.3500	1.58E-01	1.44E-01	6.40E-02	5.70E-02	5.10E-02	2.08E-02	2.04E-02	8.12E-03
1.3500 to 1.3050	1.12E-01	1.01E-01	8.23E-02	4.83E-02	6.38E-02	4.15E-02	8.18E-03	4.06E-03
1.3050 to 1.2600	1.38E-01	9.13E-02	6.40E-02	4.83E-02	1.28E-02	4.57E-02	1.64E-02	1.22E-02
1.2600 to 1.2150	1.23E-01	9.61E-02	6.86E-02	4.83E-02	4.68E-02	2.49E-02	1.23E-02	2.03E-02
1.2150 to 1.1700	8.69E-02	1.06E-01	5.94E-02	7.90E-02	5.10E-02	3.74E-02	1.23E-02	1.22E-02
1.1700 to 1.1250	1.69E-01	5.29E-02	7.31E-02	4.83E-02	4.68E-02	2.49E-02	3.27E-02	4.06E-03
1.1250 to 1.0800	9.20E-02	8.65E-02	5.94E-02	3.95E-02	3.83E-02	3.74E-02	1.64E-02	4.06E-03
1.0800 to 1.0350	1.07E-01	8.65E-02	9.14E-02	4.83E-02	3.83E-02	2.49E-02	1.64E-02	8.12E-03
1.0350 to 0.9900	7.67E-02	8.65E-02	5.48E-02	4.39E-02	3.40E-02	2.08E-02	4.09E-03	8.12E-03
0.9900 to 0.9450	1.07E-01	6.25E-02	3.20E-02	3.51E-02	3.83E-02	8.31E-03	1.23E-02	0.0
0.9450 to 0.9000	6.13E-02	7.69E-02	5.94E-02	3.51E-02	1.28E-02	2.08E-02	1.64E-02	1.22E-02
0.9000 to 0.8550	9.71E-02	6.73E-02	7.77E-02	5.70E-02	2.98E-02	1.25E-02	1.64E-02	0.0
0.8550 to 0.8100	5.11E-02	7.69E-02	4.11E-02	4.39E-02	5.10E-02	1.25E-02	4.09E-03	4.06E-03
0.8100 to 0.7650	5.62E-02	6.73E-02	3.20E-02	4.39E-02	2.55E-02	2.49E-02	1.23E-02	0.0
0.7650 to 0.7200	5.11E-02	6.25E-02	2.74E-02	1.76E-02	8.50E-03	1.25E-02	8.18E-03	4.06E-03
0.7200 to 0.6750	5.11E-02	3.85E-02	4.11E-02	1.32E-02	2.13E-02	4.15E-03	4.09E-03	0.0
0.6750 to 0.6300	7.15E-02	6.25E-02	4.57E-03	2.63E-02	2.55E-02	1.25E-02	1.23E-02	0.0
0.6300 to 0.5850	3.07E-02	3.85E-02	1.37E-02	2.63E-02	2.13E-02	8.31E-03	1.23E-02	4.06E-03
0.5850 to 0.5400	2.04E-02	1.92E-02	1.83E-02	2.19E-02	2.13E-02	0.0	8.18E-03	4.06E-03
0.5400 to 0.4950	6.64E-02	3.85E-02	3.66E-02	1.32E-02	1.70E-02	4.15E-03	0.0	4.06E-03
0.4950 to 0.4500	4.09E-02	1.92E-02	1.83E-02	1.76E-02	0.0	4.15E-03	4.09E-03	1.22E-02
0.4500 to 0.4050	1.02E-02	3.36E-02	2.74E-02	8.78E-03	1.28E-02	8.31E-03	1.23E-02	0.0
0.4050 to 0.3600	3.07E-02	9.61E-03	3.20E-02	1.76E-02	8.50E-02	8.31E-03	4.09E-03	4.06E-03
0.3600 to 0.3150	1.53E-02	1.92E-02	2.29E-02	1.76E-02	8.50E-03	0.0	0.0	0.0
0.3150 to 0.2700	2.04E-02	2.88E-02	4.57E-03	8.78E-03	1.70E-02	4.15E-03	4.09E-03	0.0
0.2700 to 0.2250	2.56E-02	9.61E-03	0.0	1.32E-02	0.0	0.0	4.09E-03	0.0

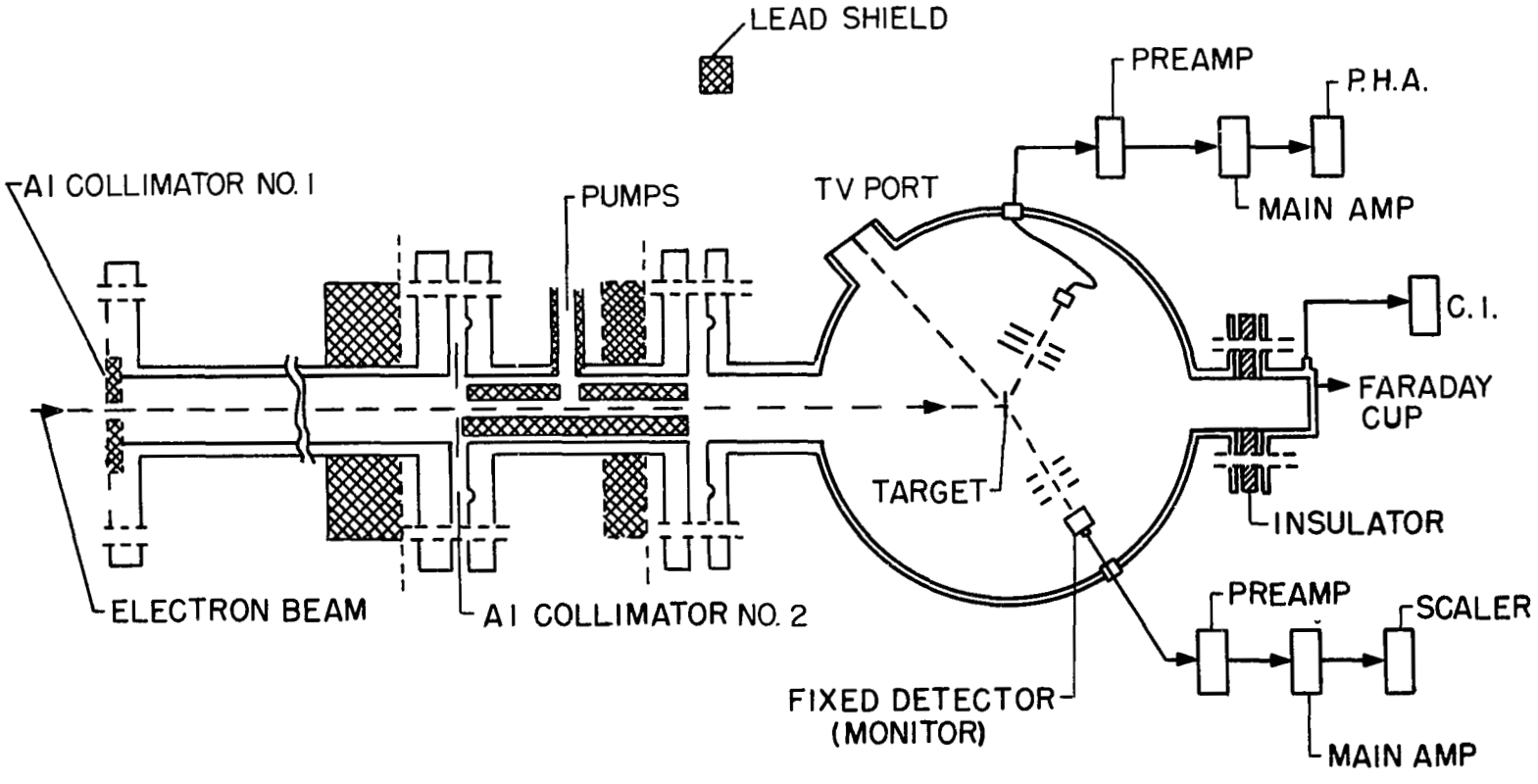

Figure 1.- Schematic diagram of the experimental setup.

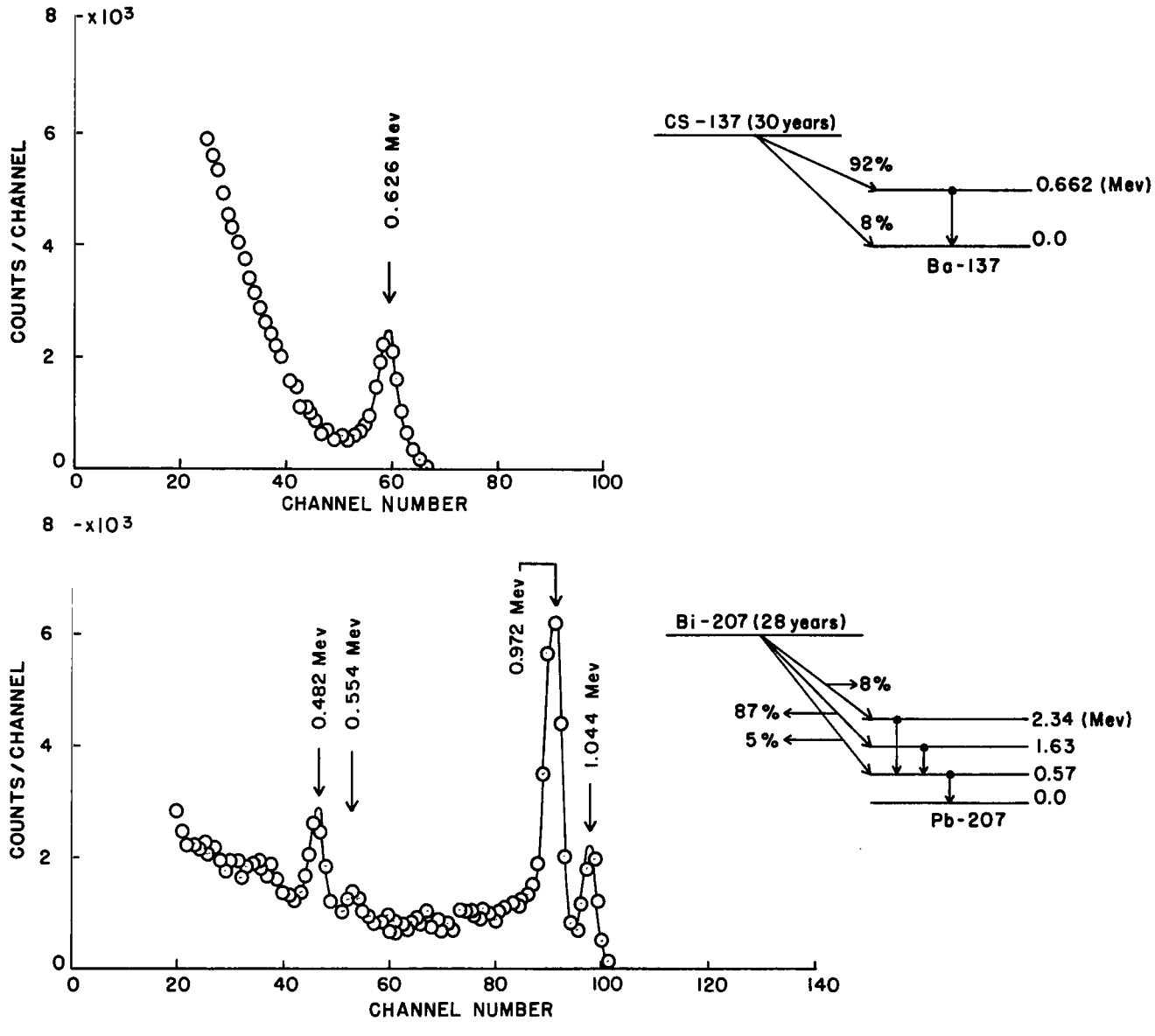

Figure 2.- Calibration spectra. Cs^{137} and Bi^{207}.

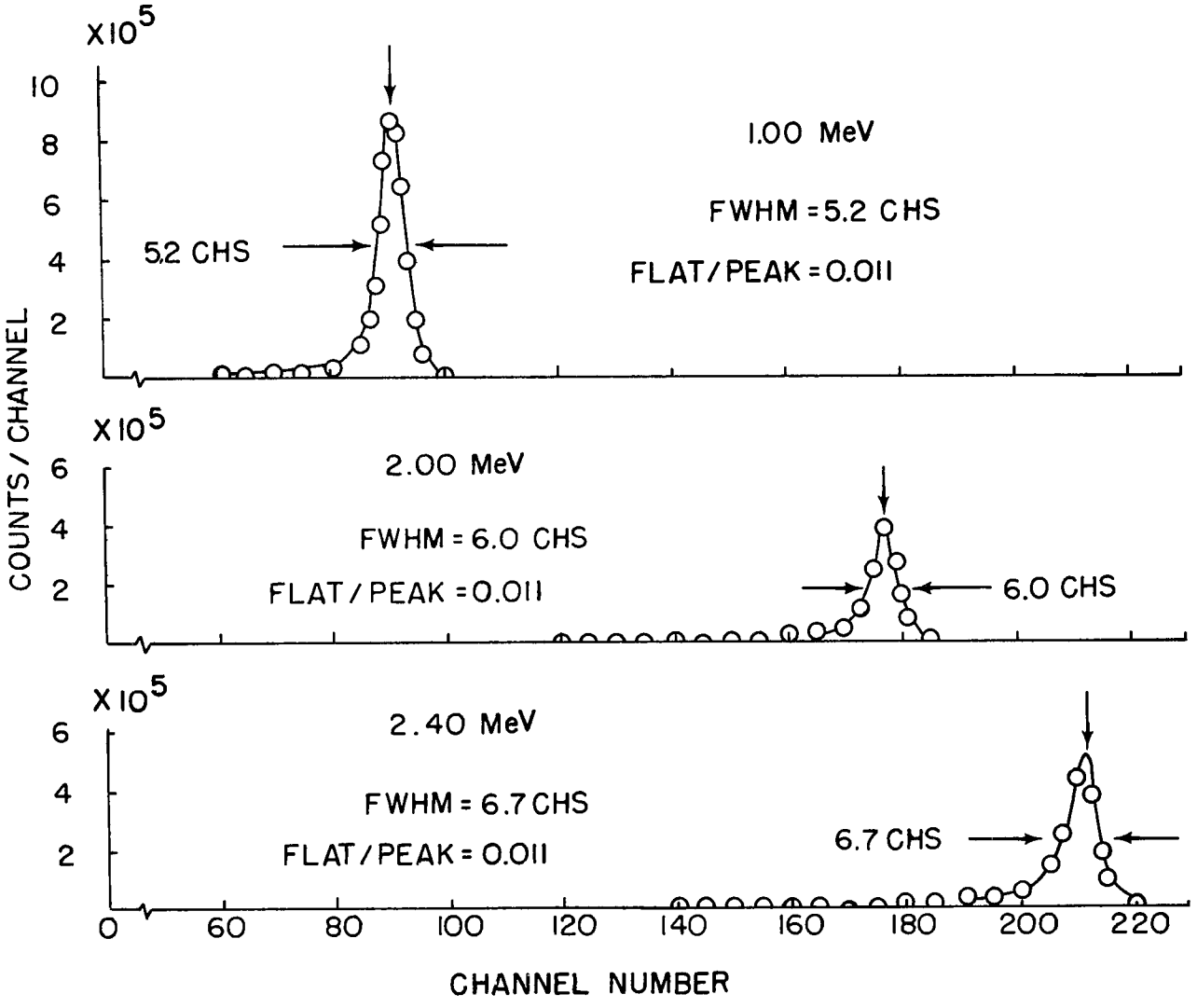

Figure 3.- Spectra of monoenergetic electrons scattered from thin (100 μg/cm^2) gold targets.

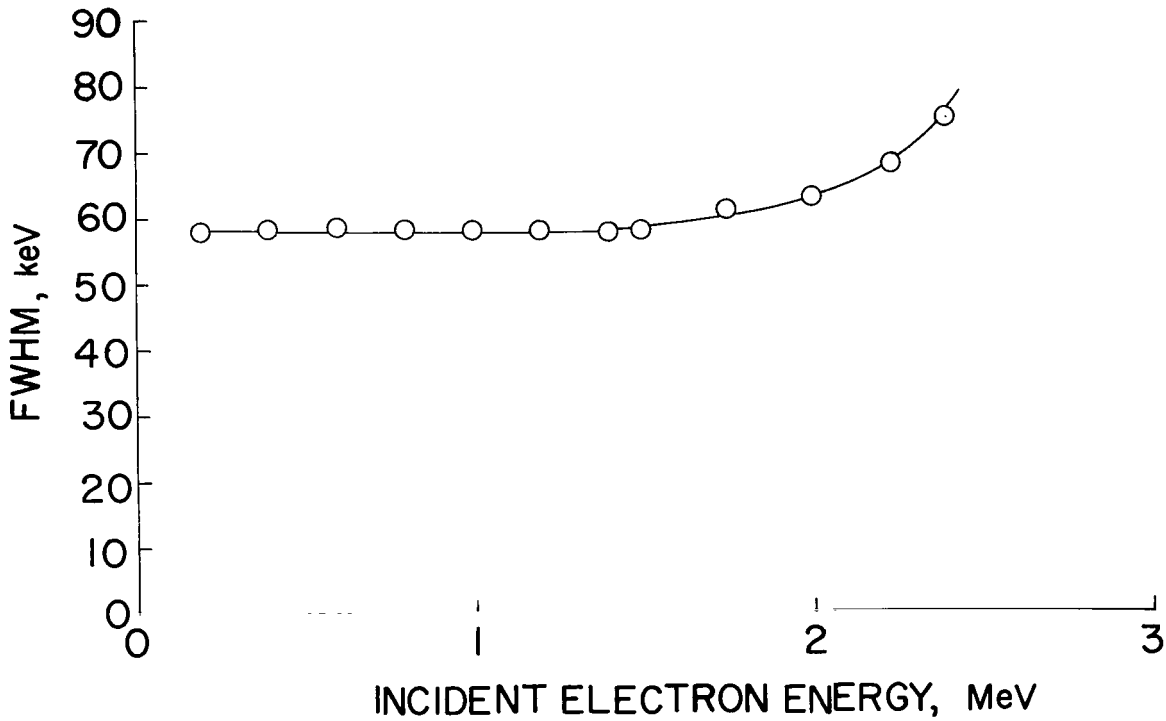

Figure 4.- Dependence of resolving power of detection system on electron energy.

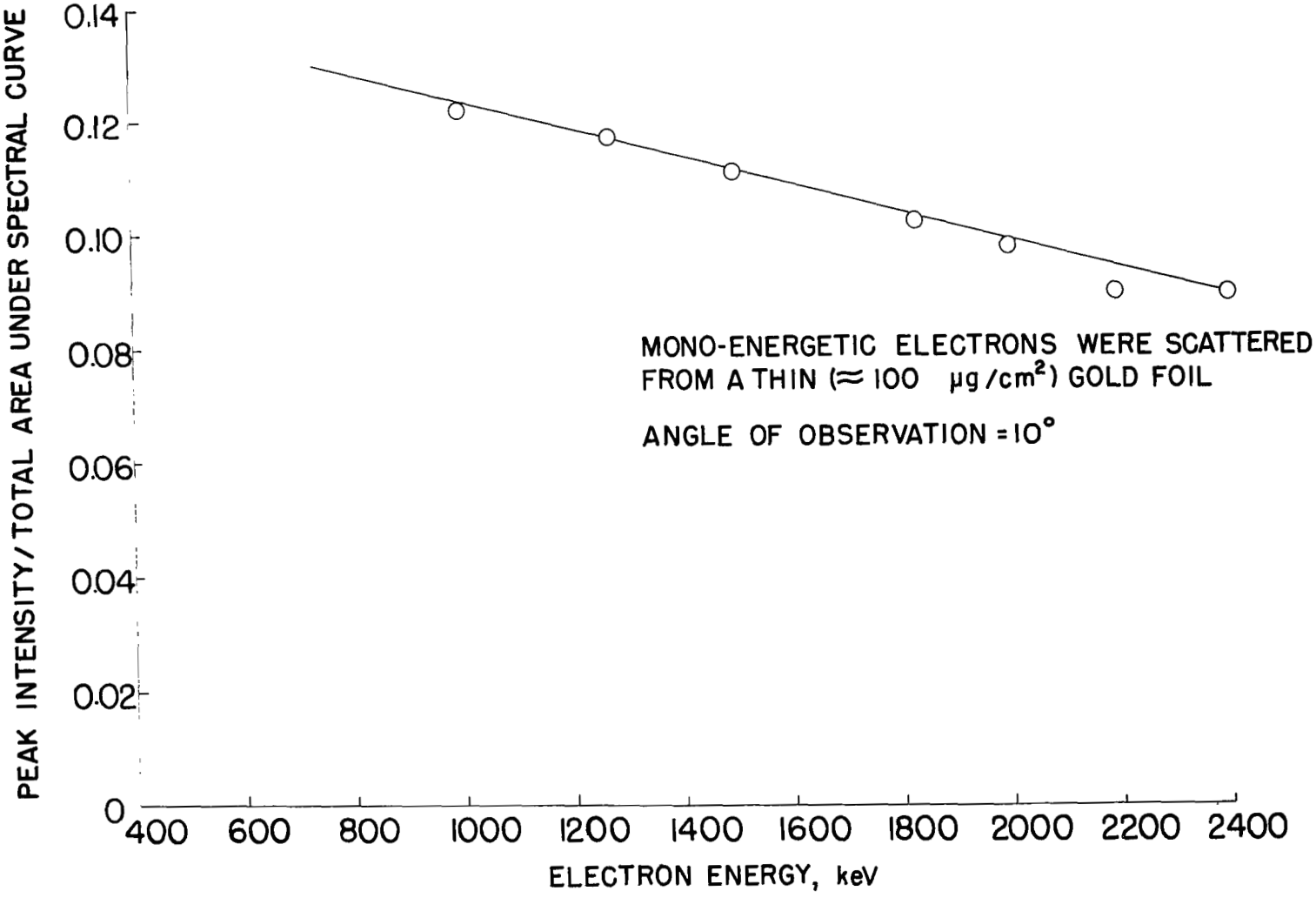

Figure 5.- Dependence of (peak intensity/total area under curve) on the electron energy.

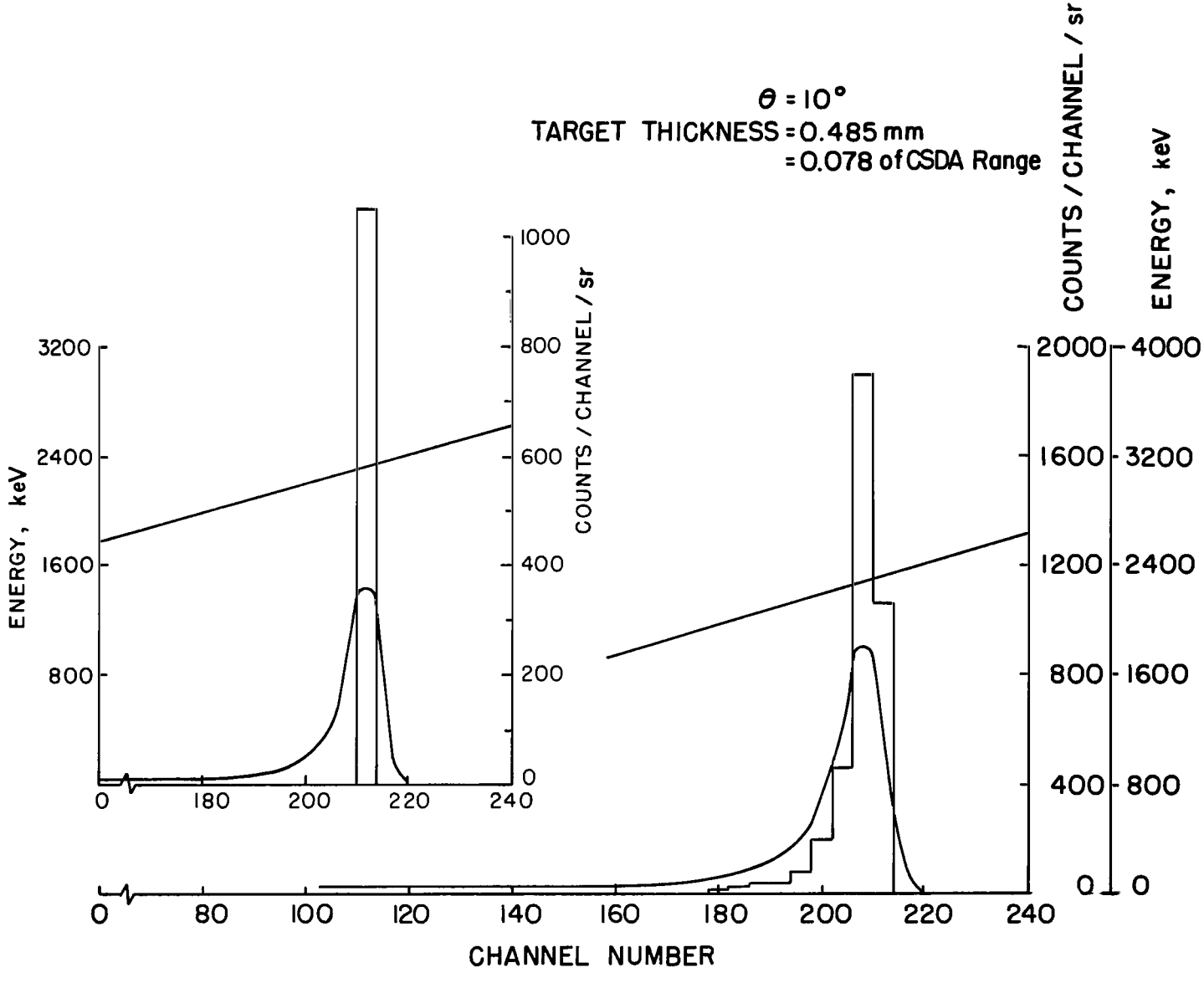

Figure 6.- Technique of modifying Monte Carlo histogram for effects of finite resolution of detection system.

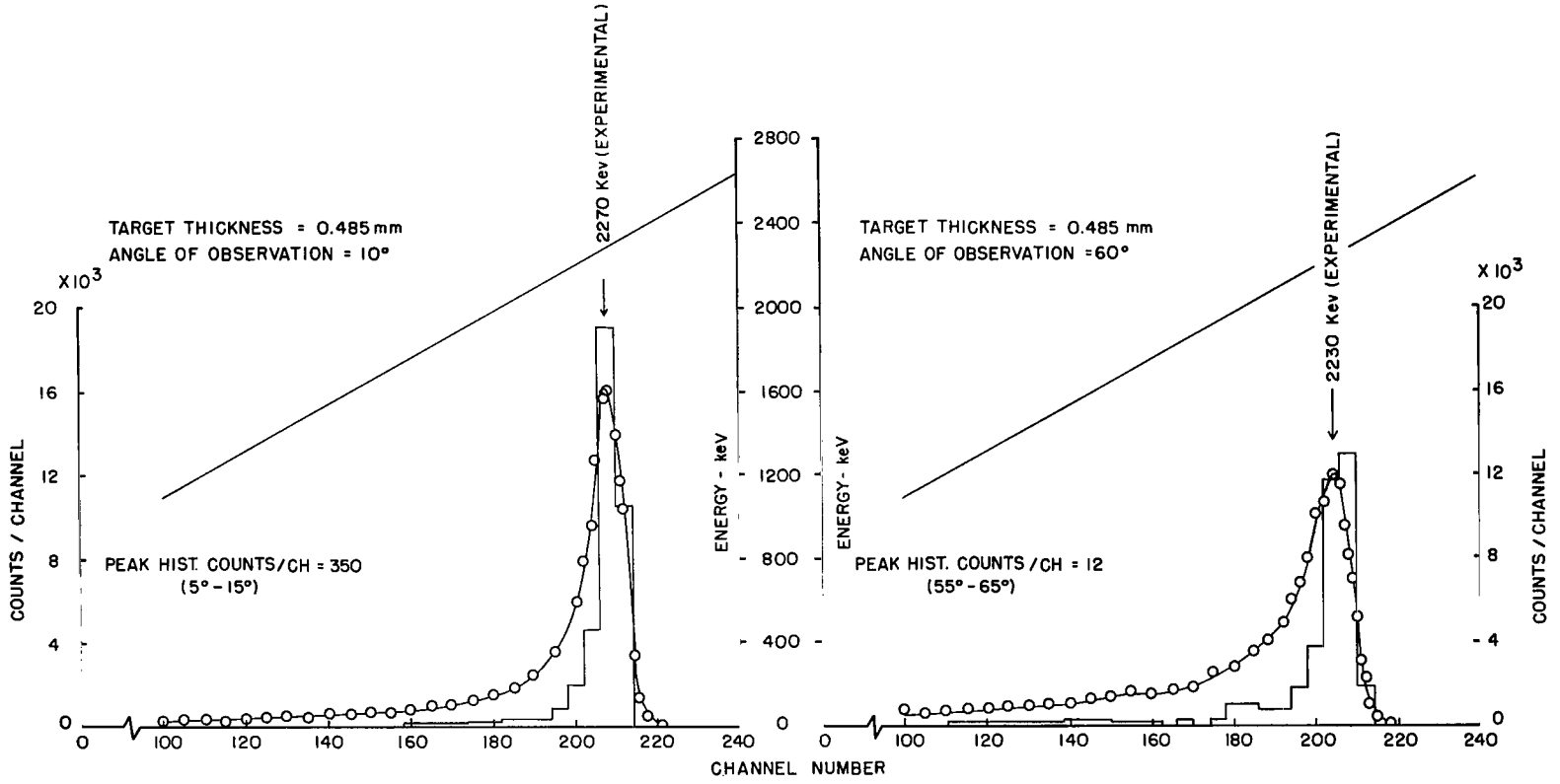

Figure 7.- Comparison between the Monte Carlo histograms and the experimentally observed energy spectra of the transmitted electrons. The Monte Carlo spectra have not been corrected for finite resolution effects.

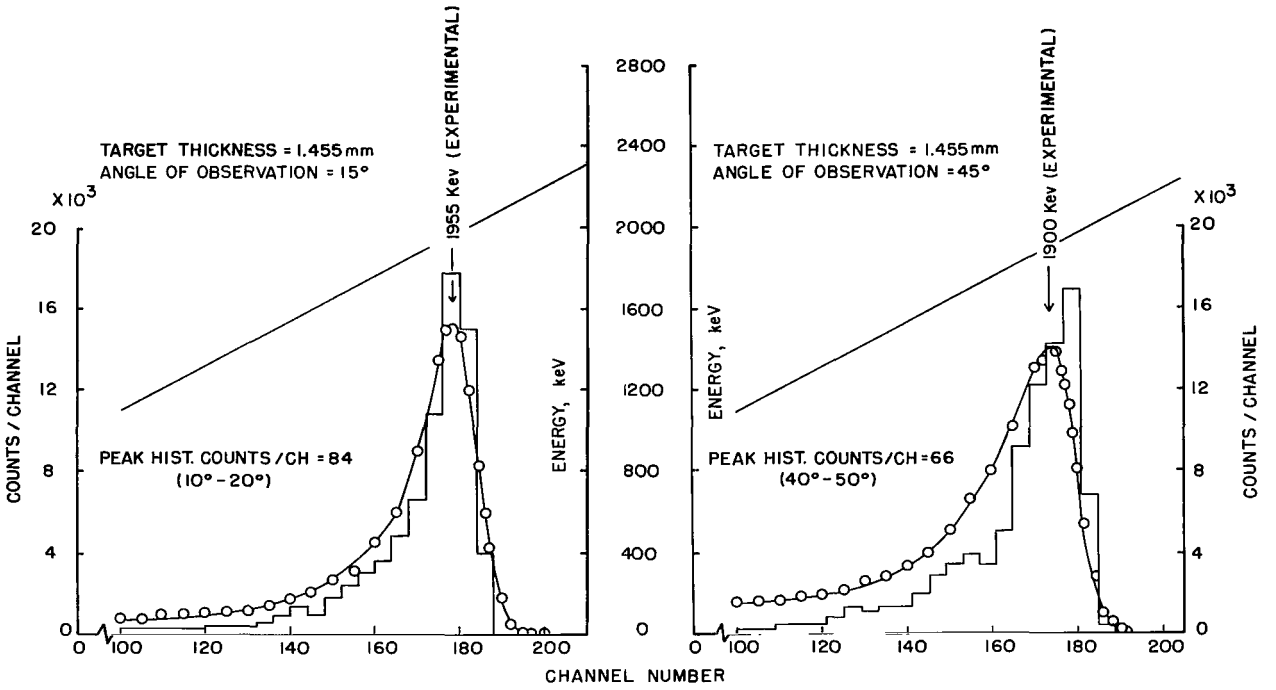

Figure 7.- Continued.

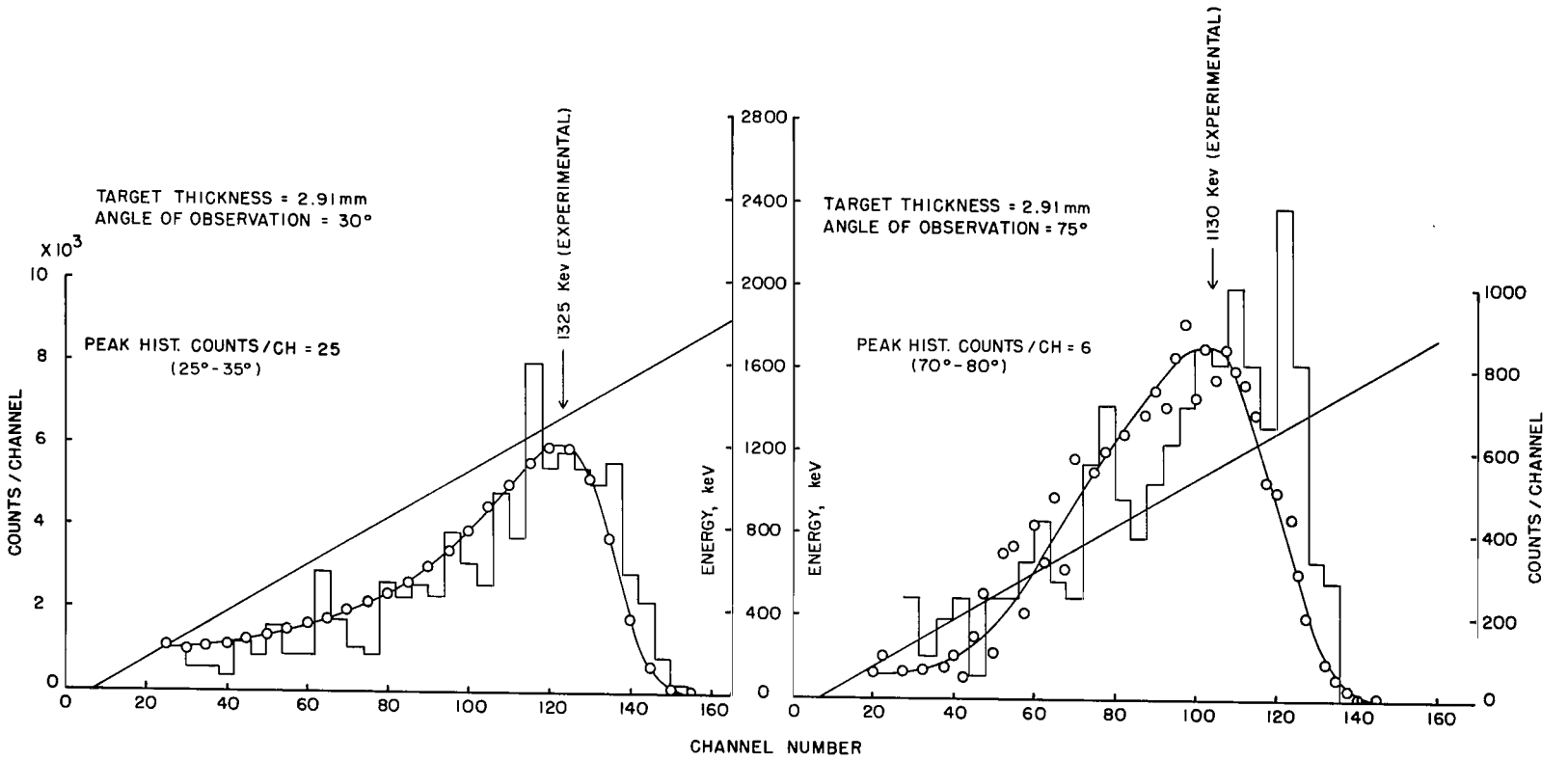

Figure 7.- Concluded.

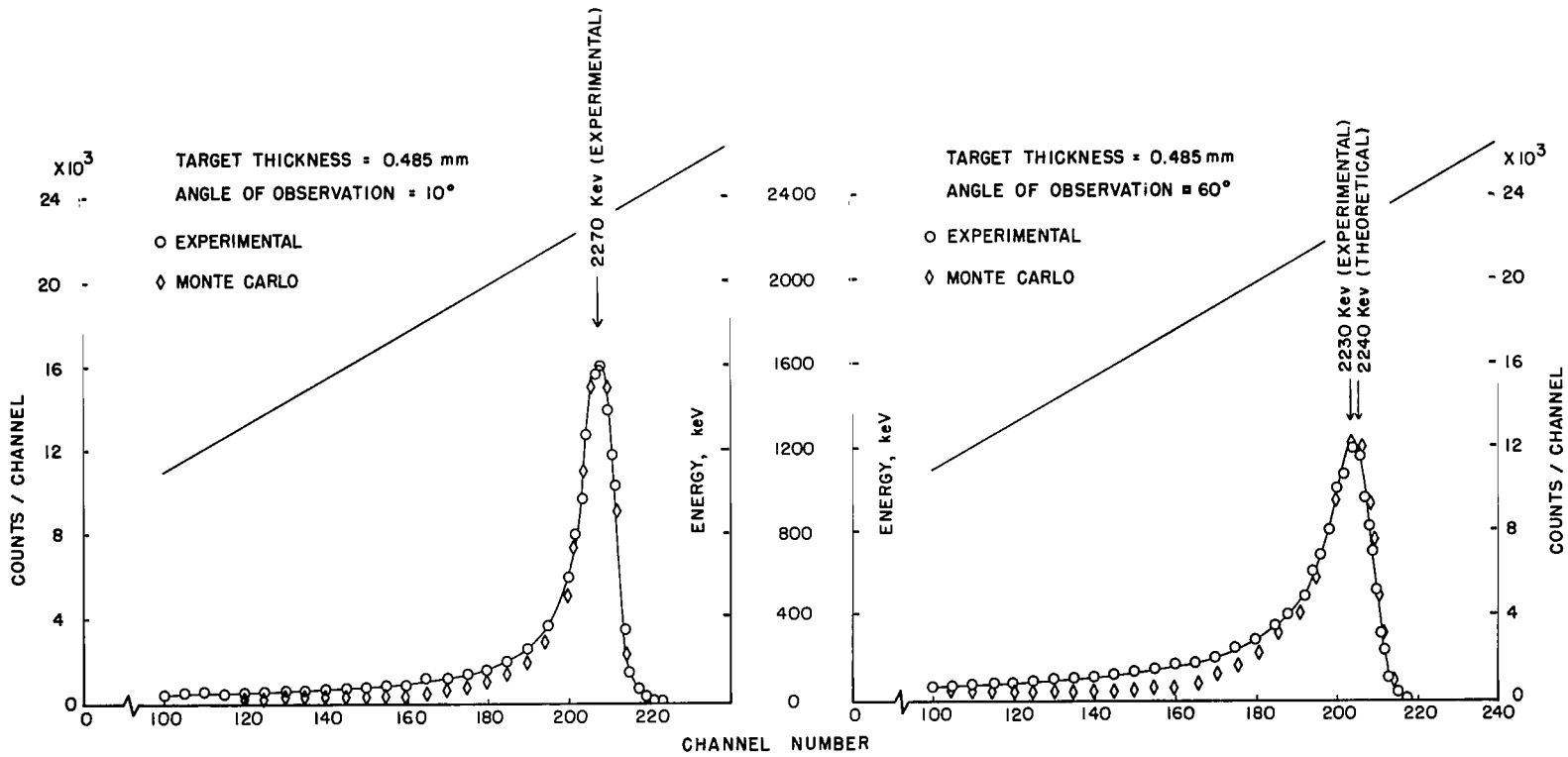

Figure 8.- Comparison of Monte Carlo spectra with the experimental data.

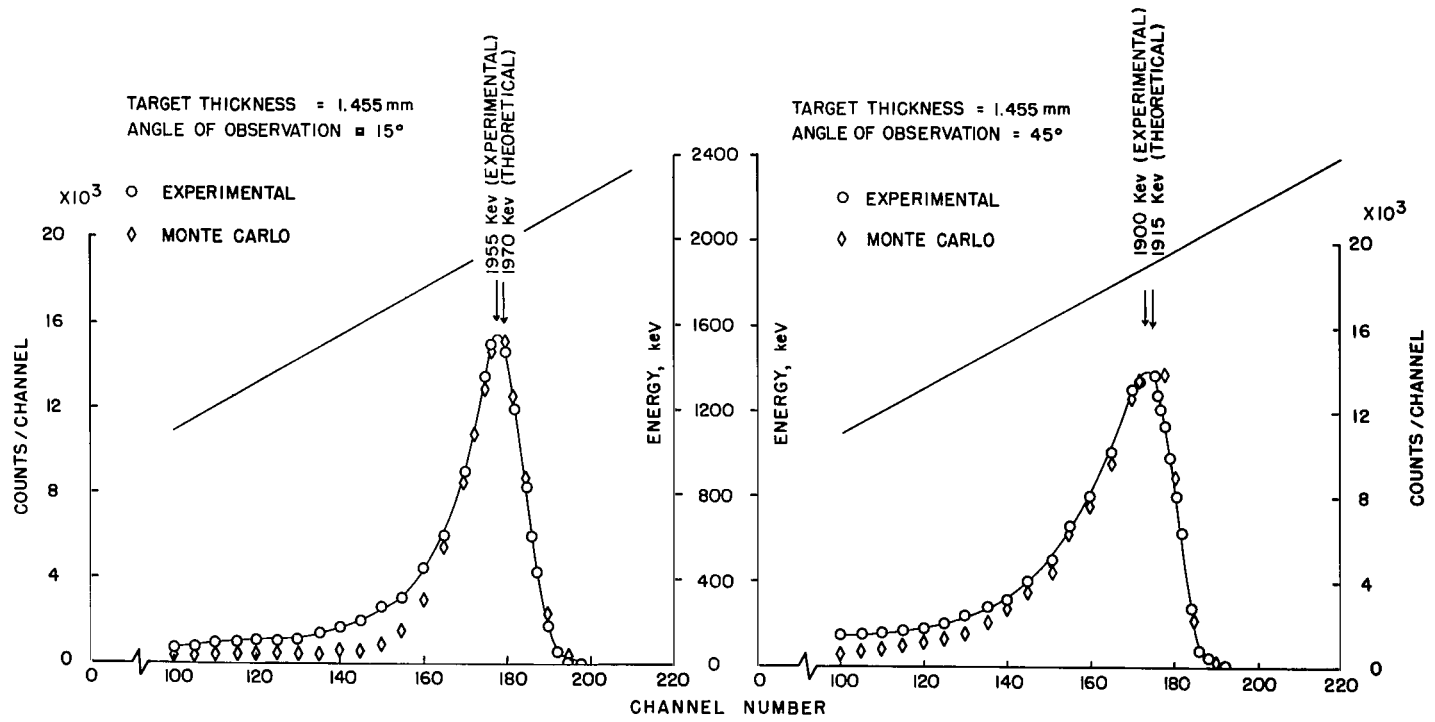

Figure 8.- Concluded.

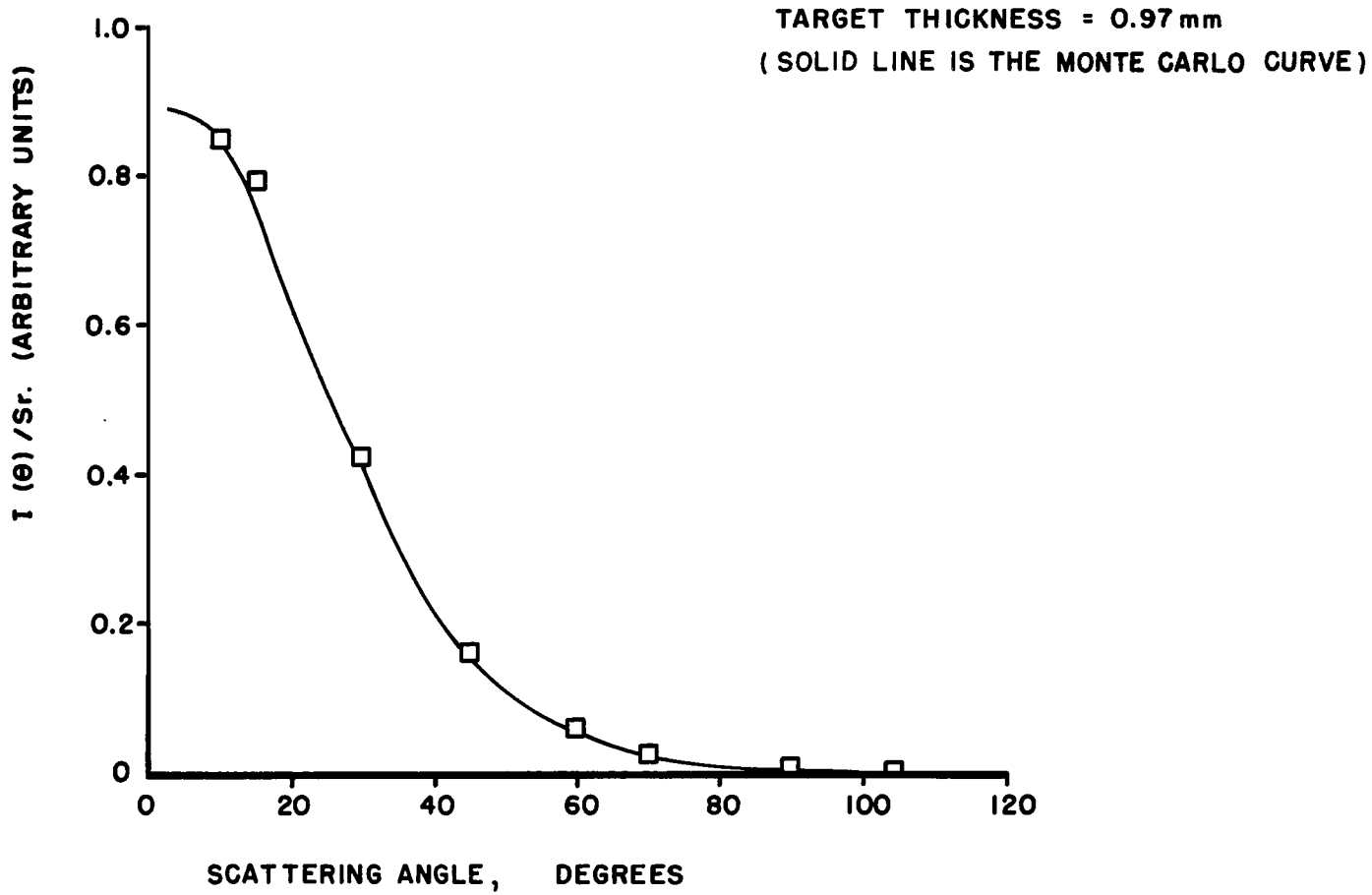

Figure 9.- Comparison of the Monte Carlo angular distribution with the experimental distribution.

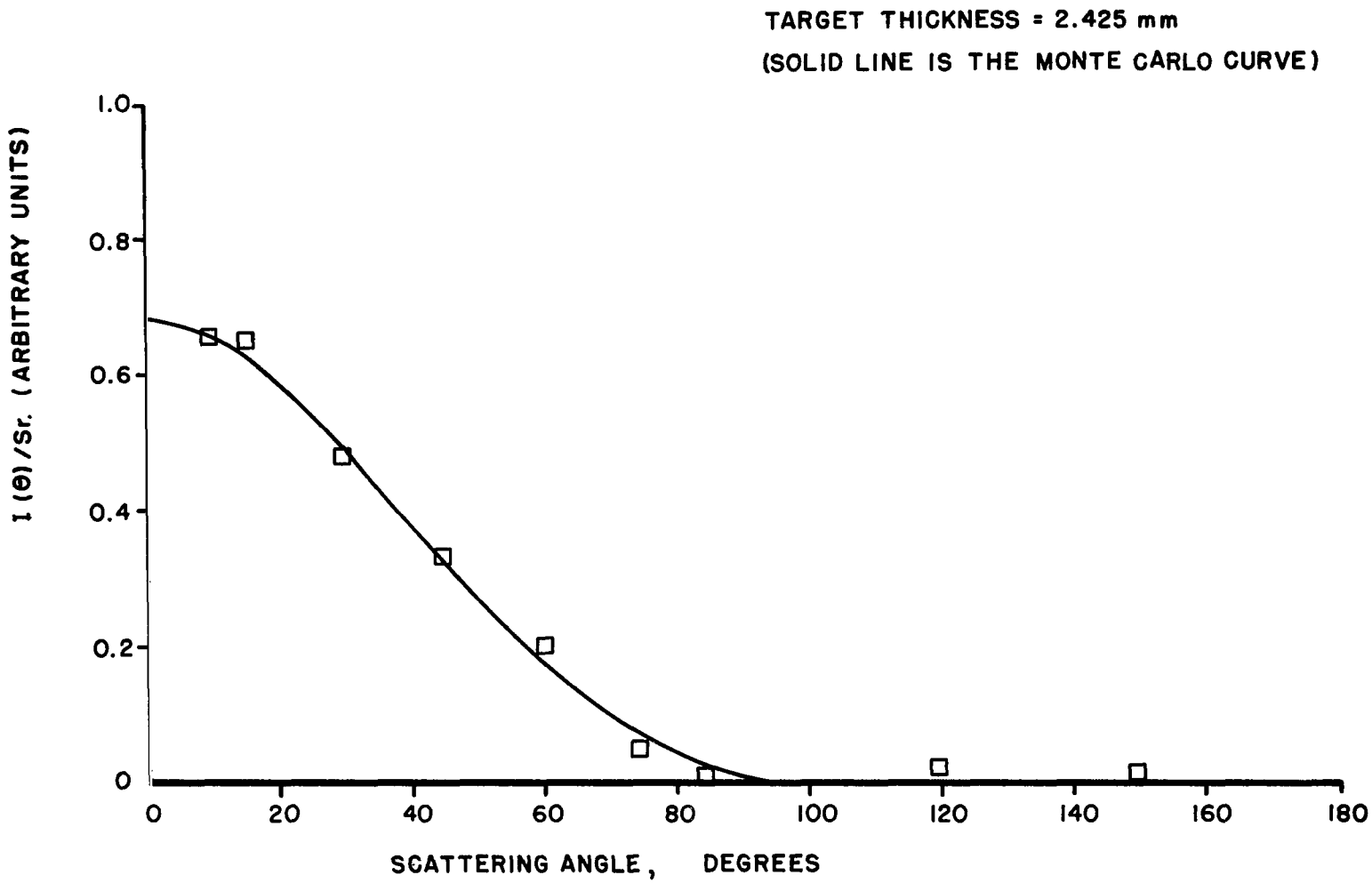

Figure 9.- Concluded.

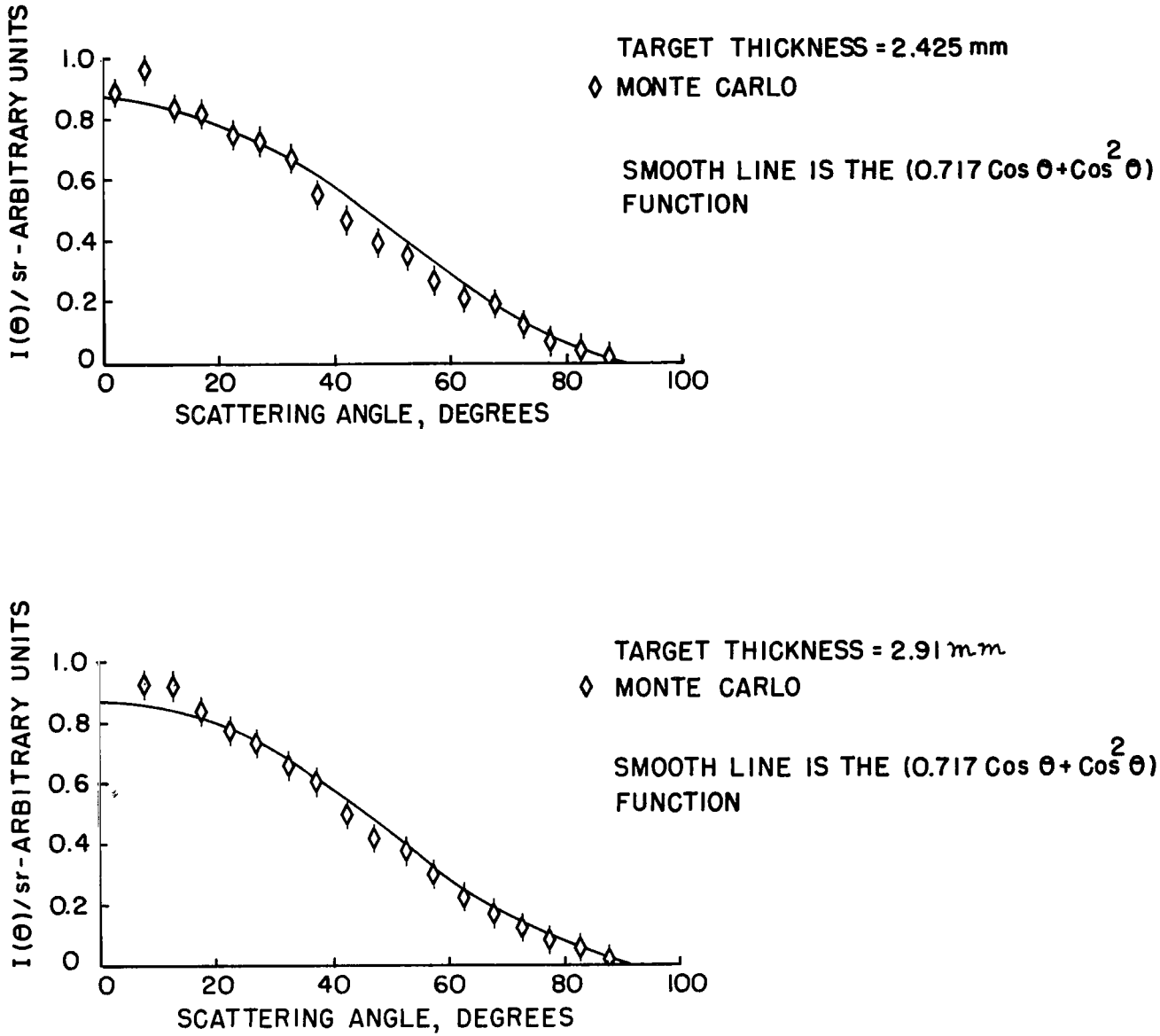

Figure 10.- Comparison of the Monte Carlo angular distribution with the Bethe function. See table I for Monte Carlo values of $I(\theta)/sr$.

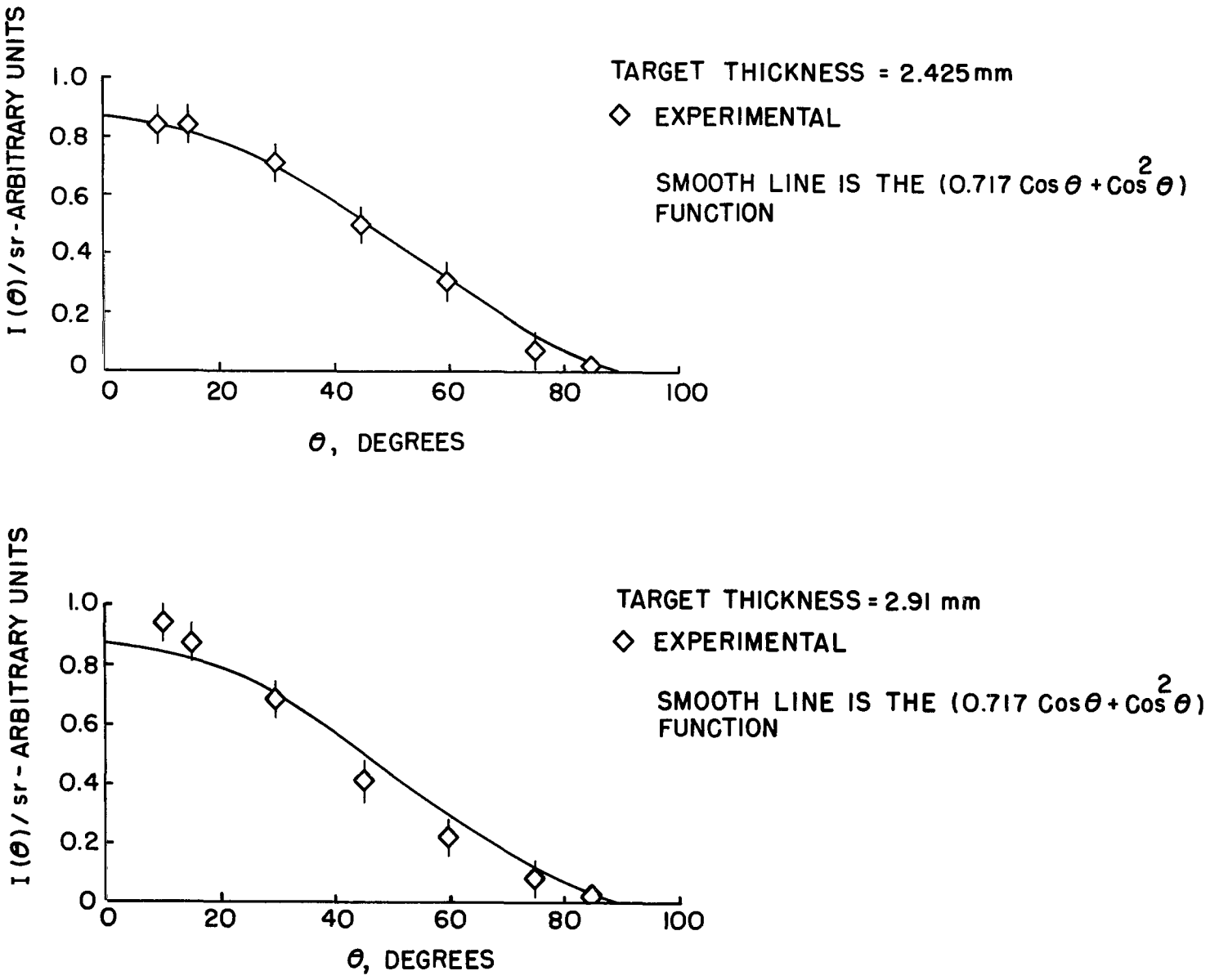

Figure 11.- Comparison of the experimental angular distribution with the Bethe function.

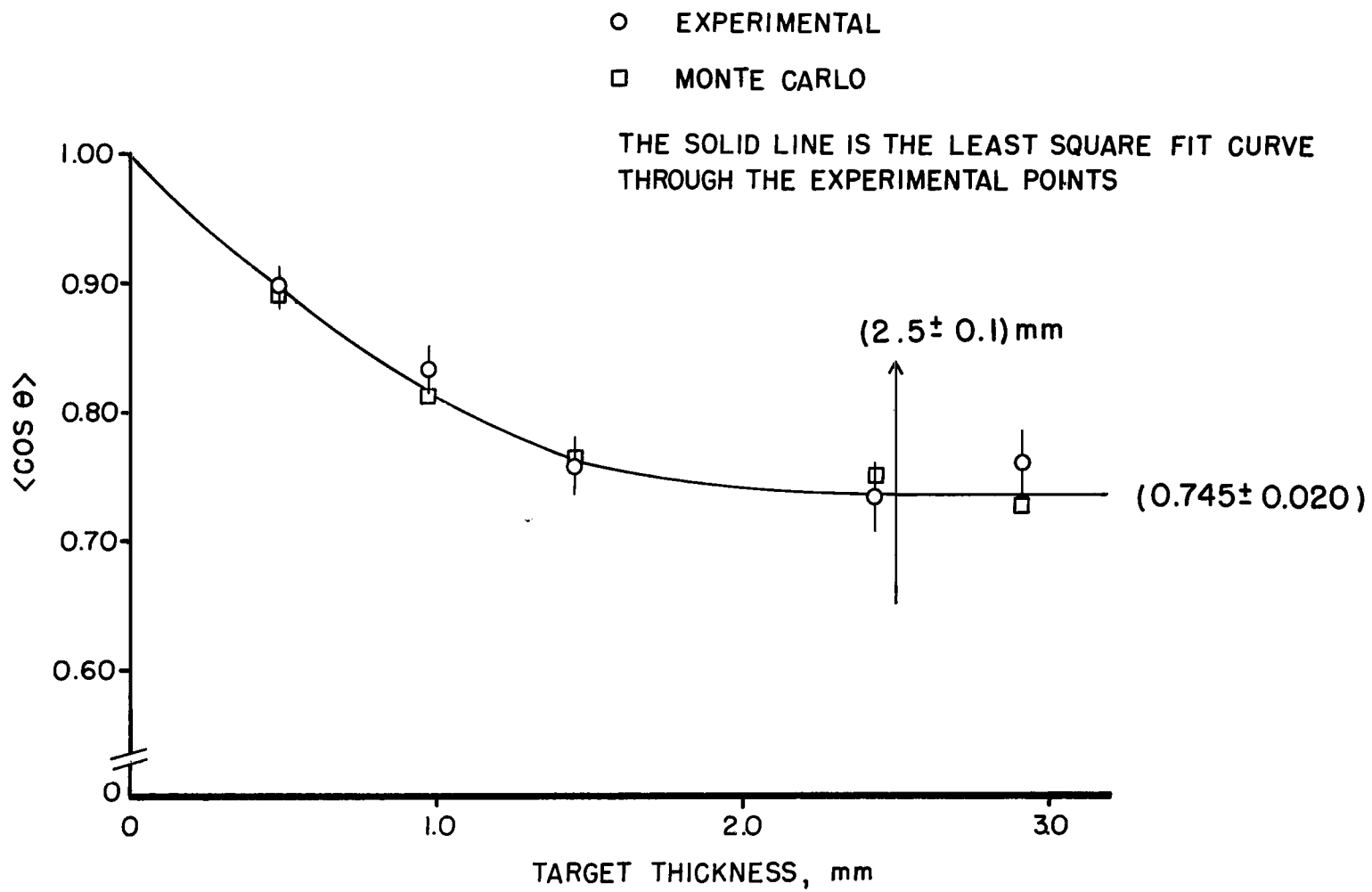

Figure 12.- Variation of average deflection of transmitted electrons with target thickness.

NATIONAL AERONAUTICS AND SPACE ADMINISTRATION
WASHINGTON, D. C. 20546

OFFICIAL BUSINESS

FIRST CLASS MAIL

POSTAGE AND FEES PAID
NATIONAL AERONAUTICS AND
SPACE ADMINISTRATION

POSTMASTER: If Undeliverable (Section 158 Postal Manual) Do Not Return

"The aeronautical and space activities of the United States shall be conducted so as to contribute . . . to the expansion of human knowledge of phenomena in the atmosphere and space. The Administration shall provide for the widest practicable and appropriate dissemination of information concerning its activities and the results thereof."

—NATIONAL AERONAUTICS AND SPACE ACT OF 1958

NASA SCIENTIFIC AND TECHNICAL PUBLICATIONS

TECHNICAL REPORTS: Scientific and technical information considered important, complete, and a lasting contribution to existing knowledge.

TECHNICAL NOTES: Information less broad in scope but nevertheless of importance as a contribution to existing knowledge.

TECHNICAL MEMORANDUMS: Information receiving limited distribution because of preliminary data, security classification, or other reasons.

CONTRACTOR REPORTS: Scientific and technical information generated under a NASA contract or grant and considered an important contribution to existing knowledge.

TECHNICAL TRANSLATIONS: Information published in a foreign language considered to merit NASA distribution in English.

SPECIAL PUBLICATIONS: Information derived from or of value to NASA activities. Publications include conference proceedings, monographs, data compilations, handbooks, sourcebooks, and special bibliographies.

TECHNOLOGY UTILIZATION PUBLICATIONS: Information on technology used by NASA that may be of particular interest in commercial and other non-aerospace applications. Publications include Tech Briefs, Technology Utilization Reports and Notes, and Technology Surveys.

Details on the availability of these publications may be obtained from:

SCIENTIFIC AND TECHNICAL INFORMATION DIVISION

NATIONAL AERONAUTICS AND SPACE ADMINISTRATION

Washington, D.C. 20546